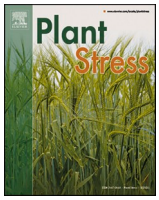
Plant Stress 19 (2026) 101200



Contents lists available at ScienceDirect

Plant Stress

journal homepage: www.sciencedirect.com/journal/plant-stress





Differential induction of autophagy and miRNA-mediated regulation modulate salt tolerance in contrasting rice varieties

Ashwini Talakayala [a], Navdeep Kaur [b], Wricha Tyagi [a], Pratap Kumar Pati [b], P.B. Kirti [c], Isha Sharma [a,d,*]

[a] International Crop Research Institute for Semi-Arid Tropics, Patancheru, Hyderabad, India-502324
[b] Department of Biotechnology, Guru Nanak Dev University, Amritsar- 143005 (Punjab), India
[c] Agri Biotech Foundation, Rajendranagar, Hyderabad, India, 500030
[d] CSIR- Central Institute of Medicinal and Aromatic Plants (CIMAP), Lucknow 226015, India

ARTICLE INFO

Keywords:
Salinity
Autophagy
Oxidative stress
Ion imbalance
miRNA regulation

ABSTRACT

Salinity stress is a major abiotic constraint to rice cultivation, limiting growth and yield worldwide. Autophagy, a conserved recycling pathway, and microRNAs (miRNAs), key post-transcriptional regulators, are emerging as central players in stress adaptation, yet their integrated roles in salinity tolerance remain unclear. Here, we compared physiological, biochemical, and molecular responses of two salt-sensitive (IR64, BPT5204) and two salt-tolerant (CSR23, Luna Sankhi) rice varieties under salinity stress. Sensitive varieties showed growth inhibition, oxidative damage, and ion imbalance, whereas tolerant varieties maintained stronger antioxidant activity, selective K^+ uptake, and osmolyte accumulation. Microscopy and gene expression analyses revealed earlier and stronger autophagy induction in sensitive lines, with differential regulation of *ATG5, ATG8d,* and *ATG12* genes. Heterologous expression of these genes in *E. coli* enhanced tolerance to salt and osmotic stress, suggesting possible non-canonical roles. Small RNA sequencing indicated salt-stress led upregulation of miRNAs in sensitive varieties targeting autophagy, ion transport, redox balance, and growth pathways. qRT-PCR validation identified *osa-miR1432-5p, osa-miR-1861e*, and *osa-miR-1874-3p* as key regulators of autophagy, redox balance, and ionic homeostasis in contrasting genotypes. Notably, *osa-miR1432-5p* is predicted to target *TOR* (Target of Rapamycin), a master autophagy regulator, providing a potential direct link between miRNA control and autophagy activation in salt-sensitive rice. These regulatory modules, together with physiological and transcriptional adjustments, distinguish the proactive tolerance of CSR and LS from the reactive stress response of IR and BPT. GO enrichment analysis revealed that BPT suppresses growth and metabolic pathways under salinity, while CSR sustains redox regulation, peroxisomal function, and ion transport, conferring superior stress tolerance. Together, these findings demonstrate that autophagy and miRNA-mediated regulation shape contrasting salinity responses in rice. Tolerant varieties appear to adopt more proactive adaptive responses, while sensitive varieties rely on rapid but costly induction of autophagy and miRNAs. These insights highlight autophagy–miRNA interactions as a potential target for engineering salt-resilient rice.

1. Introduction

Rice, the staple food for nearly half of the global population, is cultivated on over 150 million hectares, yielding approximately 543 Mt annually (Bin and Zhang et al., 2023; FAO, 2024). However, salinity stress severely threatens rice cultivation, causing yield losses of 12–50 % or more in affected regions (Chen et al., 2021; Rodríguez et al., 2023). Plants respond to salinity stress through complex and multifaceted mechanisms, including ion homeostasis, osmolyte accumulation, ROS detoxification, and metabolic reprogramming (Kaur and Pati, 2017; Hasan et al., 2024; Sharma et al., 2013). Understanding these processes is essential for developing strategies to manage salt stress effectively and safeguard future rice production.

Autophagy is an evolutionarily conserved phenomenon in eukaryotes that involves the degradation and recycling of cellular components, such as damaged organelles, aggregated proteins, and surplus

* Corresponding author.
E-mail address: ishasharma.cimap@csir.res.in (I. Sharma).

https://doi.org/10.1016/j.stress.2025.101200
Received 21 October 2025; Received in revised form 15 December 2025; Accepted 22 December 2025
Available online 24 December 2025
2667-064X/© 2025 The Authors. Published by Elsevier B.V. This is an open access article under the CC BY-NC-ND license (http://creativecommons.org/licenses/by-nc-nd/4.0/).

cytoplasmic constituents (Sharma et al., 2024). It operates at a basal level under normal conditions but is strongly induced by environmental stresses including carbon starvation, heat, drought, and salinity (Sharma et al., 2022). Autophagy led recycling of cellular constituents provides amino acids, sugars, and fatty acids that sustain metabolism and promote survival under stress (Signorelli et al., 2019). Studies in *Arabidopsis* and rice have shown that autophagy-deficient mutants are hypersensitive to drought, salt, and osmotic stress, whereas overexpression of autophagy-related genes (*ATGs*) enhances tolerance by sustaining ion sequestration, osmolyte biosynthesis, and limiting oxidative damage (Liu et al., 2009; Luo et al., 2017; Li et al., 2023). Yet, the regulation of salt-induced autophagy across rice varieties with contrasting tolerance remains insufficiently characterized. Since rice cultivars exhibit considerable genetic and physiological diversity in stress resilience (Kaur et al., 2016a; Nguyen et al., 2023; Rawal et al., 2023), genotype-specific studies are crucial to uncover how autophagy contributes to salt adaptation.

Emerging studies highlight microRNAs (miRNAs) as critical post-transcriptional regulators of stress responses, including salinity tolerance (Ding et al., 2024; Nguyen et al., 2023; Rawal et al., 2023). Studies have shown that different rice genotypes express distinct sets of salt-responsive miRNAs, which reprogram ROS homeostasis, ion transport, and metabolic pathways, thereby shaping their contrasting salt tolerance strategies (Tong et al., 2025; Nguyen et al., 2023; Goswami et al., 2017; Parmar et al., 2020). For instance, salt-responsive miRNAs such as *osa-miR393, osa-miR396b* and *osa-miR398* have been implicated in modulating root architecture, Na^+/K^+ balance, and ROS detoxification, thereby shaping varietal stress tolerance strategies (Jiang et al., 2022; Yuan et al., 2024; Li et al., 2019). However, the reprogramming of known rice miRNA during a moderate salinity stress for a short treatment window remains incompletely understood.

Here, few have profiled known osa-miRNAs under a moderate salinity regime (100 mM NaCl) at a short time period (72 h) and, critically, integrated those profiles with side-by-side comprehensive physiology and molecular readouts in tolerant versus sensitive genotypes. We highlight candidate miRNAs whose predicted targets align with distinct stress-response themes (ion/ROS/metabolic pathways) in each background, presenting a hypothesis-generating leads for future studies. Specifically, we examine whether differential induction of autophagy and ATG gene expression under moderate salinity contribute to genotype-specific salt adaptation, an area that remains under-explored. By identifying stress-responsive miRNAs, with some targeting autophagy-related genes, and associated regulatory networks, this work aims to provide mechanistic insights that can be leveraged for targeted interventions. Such an integrated approach holds strong potential for engineering rice cultivars with enhanced salt tolerance and mitigating salinity-induced yield losses, thereby contributing to sustainable rice production.

2. Materials and methods

The experimental material includes two salt-sensitive (BPT5204, IR64) and two salt-tolerant (Luna Sankhi, CSR23) genotypes. BPT5204 and CSR23 were obtained from the Indian Institute of Rice Research, Hyderabad. Luna Sankhi and IR64 seeds were obtained from Central Rice Research Institute, Odisha, India and Punjab Agriculture University, Ludhiana, Punjab, India respectively. Selection of genotypes was based on available information on their high yield rate and their tolerance to stress conditions. BPT 5204 (BPT) or Sambha Mahsuri, is a mega-variety for Eastern region which carries the submergence tolerance due to incorporation of Sub1 QTL (Singh et al., 2016). Additionally, several large effect grain yield QTLs have been introgressed in this background (Rai et al., 2023). However, this variety is sensitive to several abiotic stresses including salt (Prashanth et al., 2020). IR 64 (IR) is a semidwarf indica rice variety with high quality grains and excellent palatability but shows sensitivity to salt stress (Tiwari, 2023). CSR23 (CSR) is a high-yielding, salt-tolerant rice variety with medium slender grains, produced through a three-way cross (IR64//IR4630-22-2-5-1-3/IR9764-45-2-2) at the International Rice Research Institute (IRRI), Philippines. Due to its consistent salt tolerance in the field trials over the years, it was released for cultivation in 2004 for alkaline soils of Uttar Pradesh and Haryana and the coastal saline soils of Maharashtra, Gujarat, Tamil Nadu, Kerala, and West Bengal in India. Luna Sankhi (CR Dhan405) (LS) is obtained from a cross between IR31142-14-1-1-3-2/IR71350 at IRRI. It is a medium slender, high yielding, salt-tolerant variety released for cultivation in coastal saline areas of Odisha (Pathak et al., 2019).

For the experiments, seeds were surface-sterilized under aseptic conditions by treating them with 0.1 % (w/v) $HgCl_2$ for 15 minutes, followed by a 30-second treatment in 70 % ethanol. They were then rinsed thoroughly four to five times with sterile distilled water. In a growth chamber, seeds were grown for 9 days, on filter paper lined in glass jars moistened with half-strength liquid Murashige and Skoog (½ MS) media + 3 % sucrose at 25°C with a 12/8 h light/dark cycle. After 9 days, seedlings were supplemented with either fresh ½ MS medium as non-stressed control or with fresh ½ MS liquid medium spiked with 100 mM NaCl for the stress treatment for 72h. A treatment level of 100 mM NaCl was selected based on earlier evidence demonstrating its effectiveness in distinguishing salt-sensitive (including IR64; Saini et al., 2021) from salt-tolerant rice genotypes (including Luna Sankhi; Saini et al., 2021). At this concentration, sensitive varieties exhibit marked growth inhibition, whereas tolerant varieties are able to maintain physiological function (Li et al., 2022; Jin et al., 2025; Saini et al., 2021). Samples were collected at the end of 72h. For gene expression analysis of *ATGs* and for microscopic observation of autophagy induction, samples were additionally collected at 3h post salt-treatment. Research indicates that within 3 hours of salt treatment, autophagy is significantly induced (Luo et al., 2017). Therefore, we chose to study, 3h time point to study the immediate activation and role of autophagy in early stress response, while the 72h time point was selected to evaluate the sustained impact of salt-stressed induced autophagy on plant adaptation and survival. For all physiological, biochemical, and molecular assays, non-stressed seedlings of each genotype were included as internal controls, allowing normalization within genotypes and enabling comparative analysis across the tolerant (CSR, Luna Sankhi) and sensitive (IR, BPT) cultivars.

2.1. Determination of plant growth traits

Plant growth was determined by the measurement of root and shoot length of seedlings treated with or without salt for 72h (100 mM NaCl). Leaf area was measured using a leaf area meter by Li-COR (LI-3050C Transparent Belt Conveyor Accessory). For experiments pertaining to measurement of seedling growth under the impact of autophagy inhibitors, E64 (10 μM) and wortmannin (Wort) (5 μM), inhibitors were added to the half-strength MS media along with 100 mM NaCl on the 9th day of the seedling growth. The seedlings were then allowed to grow under this condition for the next 72h and samples were analysed for root and shoot growth.

2.2. Physiological parameters

Proline (Pro) was quantified following Bates et al. (1973). **Lipid peroxidation** was assessed spectrophotometrically by detecting malondialdehyde (MDA) formed through reaction with thiobarbituric acid (Hodges et al., 1999). **Electrolyte leakage (EL)** was measured as described by Wu et al. (2017). **Relative water content (RWC)** was determined according to Barr and Weatherley (1962).**Chlorophyll content** was measured following Arnon (1949). **Superoxide radicals ($O_2^{\cdot-}$)** and **hydrogen peroxide (H_2O_2)** were detected histochemically by incubating leaves in 6 mM nitroblue tetrazolium (NBT) in 10 mM Na-citrate buffer for 8 h (for $O_2^{\cdot-}$) or 1 % 3,3-diaminobenzidine (DAB) for 6 h (for H_2O_2) under light at 25°C (Kaur et al., 2016b). Quantitative

estimation of $O_2^{\cdot-}$ and H_2O_2 was done according to the protocol of Grellet and Díaz-Ricci (2011) and Velikova et al. (2000), respectively. For protein extraction, 500 mg of fresh leaf tissue were homogenized at 4°C in 10 ml of buffer (50 mM potassium phosphate, pH 7.8; 1 mM EDTA; 1 g PVP; 0.5 % Triton X-100). After centrifugation (12,000 rpm, 20 min), total protein in the supernatant was measured by the Bradford method (Bradford, 1976) using bovine serum albumin (BSA) as a standard. The same extract was used to determine **superoxide dismutase (SOD)** activity *via* the NBT method (Giannopolitis and Ries, 1977), **peroxidase (POD)** activity by measuring guaiacol oxidation at 470 nm, and **catalase (CAT)** activity by monitoring H_2O_2 decomposition at 240 nm (Chance and Maehly, 1955). For ion analysis, 100 mg of dried leaf or root tissue were digested with a 2:1 mixture of nitric acid and perchloric acid, then analyzed for **Na^+, K^+, and Ca^{2+}** using an XP flame photometer (BWB Technologies, UK). Selective K^+ uptake in leaves was calculated as described by Jones et al. (1991).

$$Selective\ K^+ uptake = [K^+ / Na^+]\ uptake\ in\ leaf / [K^+ / Na^+]\ uptake\ in\ roots$$

2.3. Visualization of autophagy structures using MDC and LysoTracker dye

MDC and Lysotracker staining were performed following Dejonghe et al. (2019). In short, seedlings (untreated or treated with 100 mM NaCl for 3 h and 72 h) were incubated in either 50 μM monodansylcadaverine (MDC, Sigma) or 250 nM Lysotracker Red (LTR) in PBS for 30 min, then washed three times with PBS at room temperature. Root tissues were observed and photographed under a fluorescence microscope (EVOS M5000 Imaging System, Thermo Fisher Scientific). Each experiment was repeated three times (n = 10 plants per time point per variety).

2.4. qRT-PCR analysis

Total RNA was extracted from 100 mg of leaf tissue (both treated and untreated) using the Trizol method (RNAiso Plus, Takara). The purified RNA was converted to cDNA with the Prime Script RT reagent kit (Takara, Japan). Quantitative real-time PCR was then performed on a CFX96 Real-Time PCR system (Bio-Rad, USA) using PowerUP SYBR Green Master Mix (Applied Biosystems, Thermo Fisher Scientific, North America, USA) following the manufacturer's protocol. Gene expression was determined as $\log_2$ fold change using the ΔΔCT method, with actin serving as the internal reference. Primer sequences are listed in N

Supplementary Table, ST1. Gene sequences were retrieved from Xia et al. (2011) and cross-verified against the Rice Genome Annotation Project.

2.5. ATG protein expression in E. coli and assay for stress tolerance

Custom-synthesized rice autophagy genes (*OsATG5*, 1.14 kb; *OsATG12*, 282 bp; and *OsATG8d*, 264 bp) were cloned into the protein expression vector *pET28a* (Genscript) and transformed into *E. coli BL21* (DE3) cells. An empty *pET28a* vector served as the control. To assess the potentialof the corresponding gene to confer salt (NaCl) and osmotic (PEG) stress tolerance in E. coli for which, a liquid culture assay (Yadav et al., 2014) was performed. Transformed cells were cultivated at 37°C in LB medium containing Kanamycin (50 mg/mL) until the OD_{600} reached 0.6. Protein expression was induced with 1 mM IPTG, followed by incubation at 37°C for 12 hours. Next, 20 μL of induced culture were transferred into 10 mL LB containing various stress treatments (control, 100 mM NaCl, 200 mM NaCl, 5 % PEG, or 10 % PEG). Cell growth was monitored by measuring OD_{600} hourly with a Spectrophotometer (Dhanyalakshmi and Nataraja, 2021).

2.6. miRNA sequencing

For small RNA sequencing, two cultivars, CSR (tolerant) and BPT (sensitive) treated with control/NaCl (100 mM) for 72h were chosen to reflect contrasting phenotypic groups under salinity stress, while the other two cultivars (Luna Sankhi and IR64) were included in physiological and molecular analyses but not subjected to sequencing. This approach allowed us to capture miRNA-mediated regulatory differences between tolerant and sensitive backgrounds within the available resources. Small RNA (sRNA) library preparation began with 1 μg of total RNA from each biological replicate of BPT and CSR with or without 100 mM NaCl. Samples are named as BPT-C (Control), BPT-T (salt treated), CSR-C (control), and CSR-T (salt-treated). Libraries were constructed using the TruSeq Small RNA Library Preparation Kit (Illumina, USA), following the manufacturer's protocol. In total, 12 libraries were generated, 3 replicates each for BPT-C (control), BPT-T (treated), CSR-C (control), and CSR-T (treated). The libraries were then characterized *via* gel electrophoresis, and the desired cDNA constructs were purified for miRNA sequencing (150 bp paired-end) on the Illumina NovaSeq 6000 platform.

2.6.1. Analysis of miRNA sequencing data

Post miRNA sequencing, raw sRNA reads were processed using sRNA-workbench to perform adaptor trimming, length filtering (16 -35 nt), and removing redundancy from the reads (making reads FASTA unique with abundance). For profiling of known miRNA, the FASTA sequences obtained after processing clean reads were searched for homology against the miRBase v21.0 plant sequences. During this procedure, 100 % identity with no mismatches was allowed, and perfect matches were obtained. This was done using NCBI-BLAST-2.2.29+. Alignment against the reference genome *Oryza sativa Indica* was done using *bowtie-1.1.0*. miRNA abundance was estimated from read count profiles, and differential expression was assessed using the DESeq R package, considering three biological replicates for each condition (BPT-C, BPT-T, CSR-C, CSR-T). The $\log_2$ fold change was calculated as $\log_2$ (Transcript per million, TPM under salt stress/normalized TPM under control). Differential miRNAs were screened using FDR $\leq$ 0.1 and $p \leq$ 0.05. Potential targets for known miRNAs were predicted with miRanda-3.3a, applying a minimum free energy cutoff of -20 kcal/mol and alignment Score Threshold of 150. These thresholds fall within the commonly used plant range (score ≈140–155; energy ≤ -20 kcal/mol) (Formey et al., 2014).

2.6.2. Validation of expressions of miRNA

Total RNA (from three biological replicates each of BPT-C, BPT-T, CSR-C, and CSR-T) was used for qRT-PCR using Mir-X miRNA qRT-PCR TB Green® Kit (TaKaRa, Kyoto, Japan), following the manufacturer's instructions. U6 rRNA served as the internal control. Reactions were performed in triplicate (both technical and biological) on a CFX96 Real-Time PCR system (Bio-Rad, USA) using PowerUP SYBR Green Master Mix-2x (Applied Biosystems, Thermo Fisher Scientific, North America, USA). Gene expression was quantified as $\log_2$ fold change by the ΔΔCT method. Primer sequences are listed in Supplementary Table, ST1.

2.6.3. Gene Ontology (GO) analysis

GO was performed using ShinyGO 0.77 (http://bioinformatics.sdstate.edu/go/) highlighting the top GO enriched terms. The p-value was adjusted by FDR correction, and terms were deemed significantly enriched when FDR $\leq$ 0.05.

2.7. Statistical analysis

All data were analyzed using two-way or one-way ANOVA to examine genotype differences under control and 100 mM NaCl conditions. Results are shown as the mean ± SE of three independent biological replicates. Multiple comparisons were adjusted using the Bonferroni correction in GraphPad Prism 9.0, with significance set at $p \leq 0.05$.

3. Results

3.1. Impact of salt stress on growth and membrane integrity

Four contrasting cultivars of rice, *viz.* IR, BPT, CSR and LS, treated with 100 mM NaCl for 72 h, showed varied responses in morphology. All the varieties showed a significant decline in root and shoot length, though to different levels (Fig. 1). The shoot length (Fig. 1a) in IR and BPT was reduced (as % of non-saline controls) by 22 % and 26 %, while LS and CSR showed a decrease of 12 % and 15 %, respectively. Similarly, root length (Fig. 1b) was reduced by 28 % and 25 % in IR and BPT, respectively, whereas CSR and LS recorded a decline of 11 % each in comparison to control values. Interestingly, a significant decline in leaf area (Fig. 1c) was observed only in sensitive varieties, with a 26 % and 22 % decline in IR and BPT compared to their respective controls.

Salt stress in plants is often accompanied by loss of membrane integrity and ROS accumulation. We observed a significant decline in RWC under salt stress in IR and BPT, however, no change in RWC was observed in tolerant varieties (Fig. 1d). Electrolyte leakage is an indicator for membrane damage caused by salt stress. After the salt treatment, EL increased significantly to almost twice its value as compared to their respective controls in IR and BPT. CSR showed a slight increase in EL, while LS showed a non-significant increase as compared to their respective controls (Fig. 1e). Elevated levels of lipid peroxidation were reflected by a significant enhancement in MDA content by 65 % in IR and 100 % in BPT as compared to their respective controls (Fig. 1f). Similarly, a significantly enhanced MDA level by 40 % and 34 % was observed in CSR and LS as compared to their respective controls. Plants usually cope with osmotic stress through the generation of osmolytes like proline. Interestingly, the tolerant varieties showed significantly enhanced proline content as compared to sensitive varieties even under non-stressed conditions (Fig. 1g). Salt treatment resulted in the highest increase in proline content in BPT (106 %), followed by IR (87 %), CSR (38 %) and LS (76 %) in comparison to their respective controls. However, the actual values of proline content remained higher for LS (22 μg gFW^{-1}) and CSR (23 μg gFW^{-1}) as compared to IR (16.5 μg gFW^{-1}) and BPT (14.4 μg gFW^{-1}) under saline conditions.

3.2. Impact of salt stress on redox status and ion homeostasis

We analysed the ROS accumulation through the histochemical staining of the total H_2O_2 and $O_2^{\cdot-}$ production (Fig. 2a and b). The images showed that the staining for $O_2^{\cdot-}$ (NBT staining) and H_2O_2 (DAB staining) was darker for sensitive varieties than the tolerant varieties under salt stress. Further concurrence on these results came from the biochemical estimation of $O_2^{\cdot-}$ (Fig. 2c) and H_2O_2 (Fig. 2d) accumulation that supported that under salt stress IR and BPT showed a significantly increased $O_2^{\cdot-}$ levels by 84 % each as compared to a 48 % increase in LS and a non-significant increase in CSR with respect to their control values. Similarly, H_2O_2 content also increased (as % of non-saline controls) to 180 % and 152 % in IR and BPT, respectively whereas CSR and LS also showed around a 55 % increase each. To determine the ROS scavenging potential of the plants under stress, we analysed the enzyme activity of three prominent antioxidant enzymes *viz.* SOD, POD and CAT. Under salt stress, SOD activity (Fig. 2e) increased significantly to 28 % and 38 % in IR and BPT (as % of non-saline controls). CSR and LS recorded an increase of 79 % and 64 % respectively in SOD activity as compared to their respective controls. In the case of POD (Fig. 2f), a significant

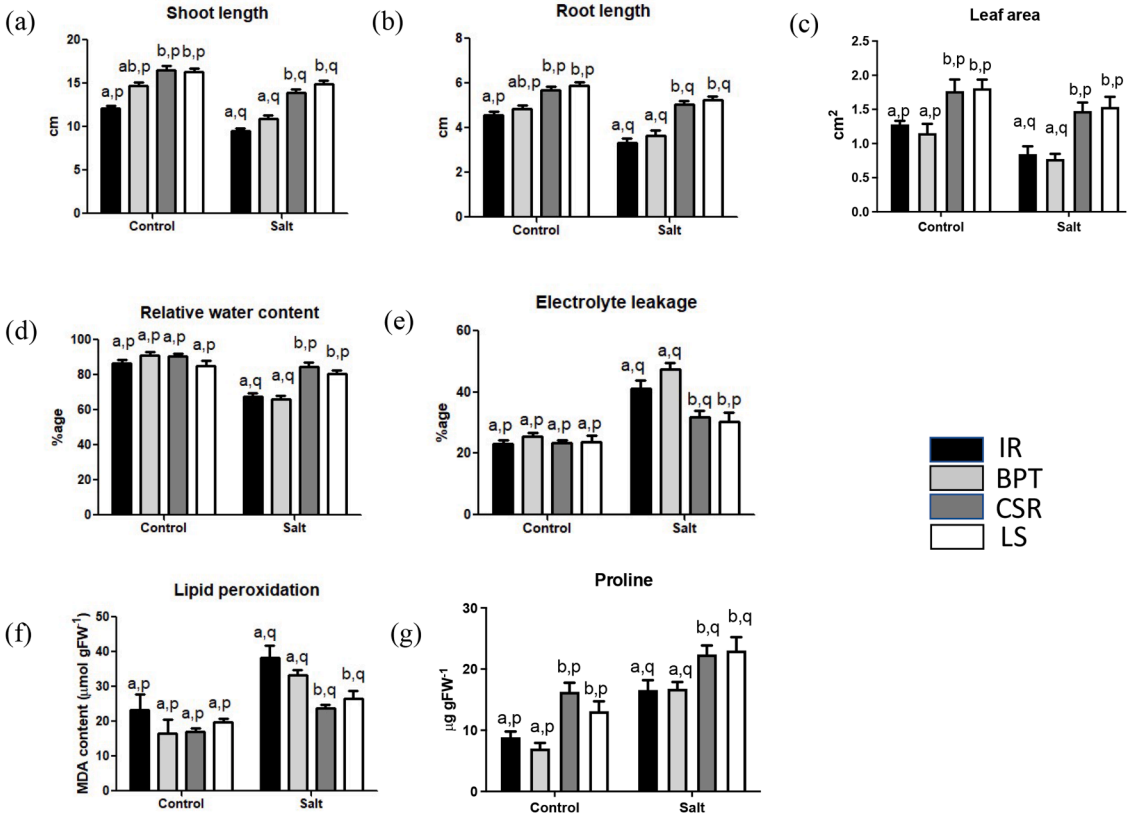


Fig. 1. Morphological differences of four rice genotypes (BPT, IR, CSR and LS) grown under 100 mM of NaCl. Seeds were grown for 9 days in glass jar and seedlings were treated with either MS medium as a control (non-stressed) or with MS liquid medium supplemented with 100mM NaCl (stressed) for 72h. Graphs (a)-(c) represent change in shoot and root length and leaf area (n =20). Graphs (d)-(g) represent relative water content, electrolyte leakage, lipid peroxidation (MDA content) and proline content. Values are represented as Mean ± SE of three independent biological and three technical replications. Different lowercase letters (a–d) indicate statistically significant differences among genotypes, whereas different lowercase letters (p and q) denote significant differences between control and salt-treated samples within each genotype ($p < 0.05$).

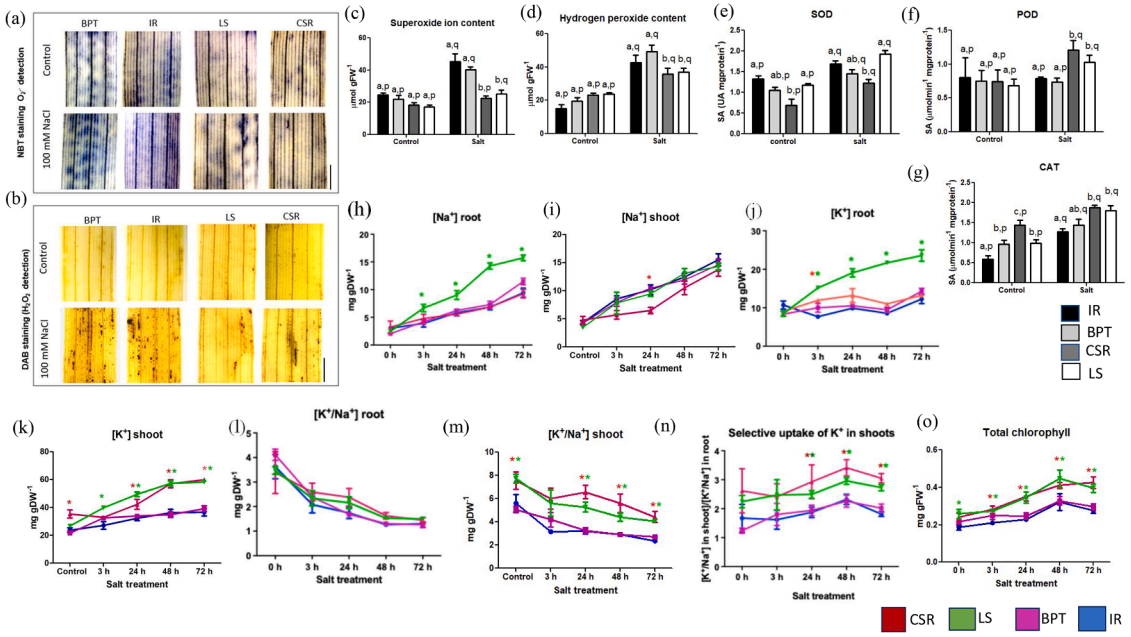


Fig. 2. Histochemical detection of ROS in leaves of rice genotypes inflicted with salinity stress (100mM NaCl) for 72h. (a) NBT staining indicating O_2^- and (b) DAB indicating H_2O_2 in leaves of rice is captured as dark stained patches on the leaves. Histograms represent biochemical estimation of (c) O_2^- (d) H_2O_2, specific activity of antioxidant enzymes (e) superoxide dismutase (SOD), (f) guaiacol peroxidase (POD), (g) catalase (CAT) in rice leaves under salinity stress for 72h. Values are represented as Mean ± SE of three independent biological and three technical replications. Different lowercase letters (a–d) indicate statistically significant differences among genotypes, whereas different lowercase letters (p and q) denote significant differences between control and salt-treated samples within each genotype ($p < 0.05$). (h-o) Na^+, K^+ contents, K^+/Na^+ ratio, selective K^+ uptake and chlorophyll content in rice genotypes inflicted with salinity stress (100mM NaCl) for 72 h. Samples were collected at 3, 24, 48 and 72h after salt stress. The asterisks * represent significant change at $p<0.05$ in comparison to one of the sensitive varieties (BPT) at all time-points. The values presented are the mean ± SE of three independent biological and three technical replications.

increase in activity was recorded only in tolerant varieties CSR and LS with 62 % and 50 % increase respectively as % of non-saline controls. CAT activity increased in all the varieties in response to salt stress and led to a significant increment in IR (35 %), BPT (40 %), CSR (31 %) and LS (82 %) as compared to their respective controls (Fig. 2g).

To analyse the impact of salinity stress on ionic balance, we performed a time scan analysis of ion uptake in all the varieties under salinity stress. We found that salt treatment resulted in almost a linear increase in root Na^+ uptake from 3h to 72h in all the varieties (Fig. 2h). However, LS showed a significantly higher Na^+ uptake as compared to the rest of the varieties from 3h to 72h. For instance, the root Na^+ uptake was 15.7 mg gDW^{-1} in LS that differed significantly from BPT that accumulated 11.4 mg gDW^{-1} Na^+ at 72h. Though shoot Na^+ accumulation also increased consistently in all the varieties (Fig. 2i), shoot Na^+ at 24 h in CSR (6.4 mg gDW^{-1}) was significantly lower as compared to BPT (10.16 mg gDW^{-1}) which showed no significant difference with other varieties. Interestingly, LS showed a linear increase in K^+ uptake in roots from 3 to 72h as compared to BPT which did not differ significantly from other varieties (Fig. 2j). For instance, root K^+ uptake (Fig. 2j) in LS was 23.6 mg gDW^{-1} as compared to 14.2 mg gDW^{-1} in BPT at 72 h. Interestingly, shoot K^+ uptake in tolerant varieties was significantly higher than that observed in sensitive varieties at 24 h and beyond (Fig. 2k). In roots, K^+/Na^+ uptake ratio decreased in all the varieties with no significant difference (Fig. 2l), whereas in shoot, K^+/Na^+ uptake (Fig. 2m) in tolerant varieties was significantly higher than in the sensitive varieties at 24h and beyond.

It was interesting to see that the selective K^+ transport was significantly higher in the tolerant varieties than the sensitive varieties at 24h and beyond of the salt treatment (Fig. 2n). We also looked at the total chlorophyll content under the similar time scan experiment to assess chlorophyll degradation with increasing Na^+ concentration, which is an indication for tissue tolerance. Change in chlorophyll content of all the varieties followed a similar trend but the values of chlorophyll content were significantly higher in tolerant than in the sensitive varieties at 24h and after (Fig. 2o).

3.3. *Autophagy is induced under salt stress in rice cultivars*

3.3.1. *Induction of autophagic puncta and acidification of cellular compartments*

Autophagy is often induced under stressful conditions to help the plant cope up with deformed proteins and macromolecules. It can be elicited as an early or late stress response. Therefore, we attempted to analyse the accumulation of autophagosomes at 3h and 72h after salt stress. As the mature autophagosomes have an acidic lumen, they can accumulate acidotropic fluorescent dyes, such as MDC and LTR. MDC staining of the roots of all varieties revealed several MDC-stained puncta as compared to their respective controls. Live-cell imaging revealed that they are more abundant in sensitive varieties than in the tolerant ones (Fig. 3a). These puncta were observed as early (3h) as well as late stress responses (72h). Using LTR staining, in comparison to control, we could observe several acidic cells in the roots of the salt-treated plants (Fig. 3b). Moreover, cellular acidification looked visibly more intense in sensitive varieties as compared to the tolerant lines at both 3 and 72h post-stress.

3.3.2. *Salinity induced changes in the expression of OsATGs and salt stress responsive genes*

We analysed the expression of several key autophagy related (16*OsATGs*and *TOR)* and salt stress related genes(*OsLEA, OsP5CS1, P5CS2* and *OsSalT*) in response to early (3h) and late (72h) salt stress conditions in both the tolerant and sensitive cultivars (Fig. 4a and b). After 3 h salt treatment in IR, a significant downregulation of expression was observed in *ATG1a* (0.2-fold), *4a* (5.3-fold), *4b* (5.6-fold), *5* (2.15-fold), *8c* (5.1-fold), *10* (3.7-fold),*13b* (3.1-fold)*TOR* (2.7-fold) and a significant upregulation was observed in *ATG3a* (1.5-fold), *7* (2.5-fold),

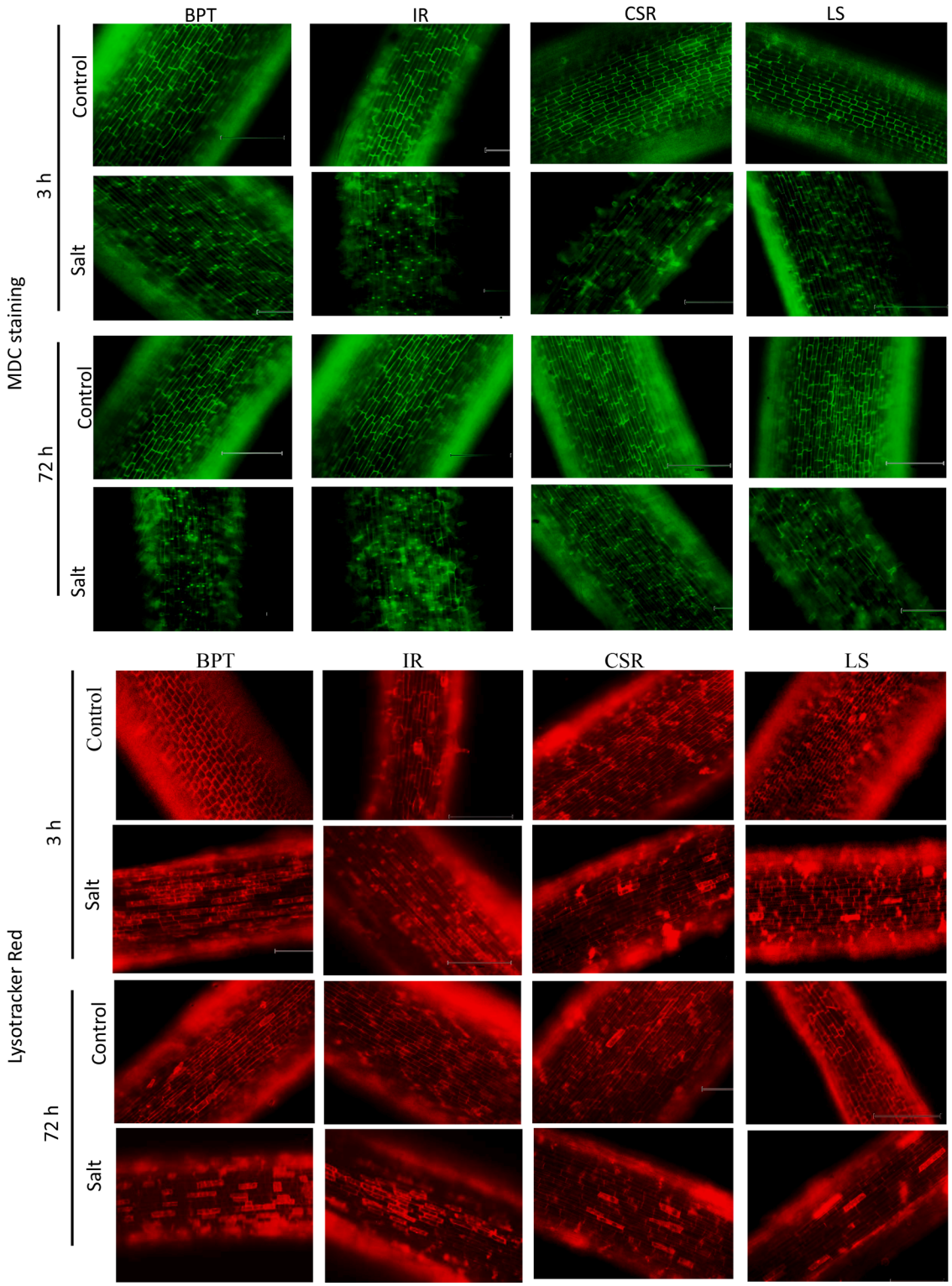


Fig. 3. (a) MDC staining (b) Lysotracker staining depicting autophagic puntae and acidic cells in roots of rice genotypes treated with salinity (100mM NaCl) for 3 and 72h. The experiment was performed as three independent biological replicates (n=10). Scale bar=150 μm.

8b (1.9-fold), *8d* (1.9-fold), *8e* (1.8-fold), *ATG9a* (2.3-fold) as compared to respective controls.

After 72h of salt treatment, *ATG 7* (1.7-fold), *8a* (2.8-fold), *8c* (3-fold), *8d* (2.9-fold), *8e (2.7-fold), 9a* (4-fold), *13b* (1.5-fold), *18f* (2.4-fold) were significantly upregulated while *ATG5* (2-fold), 12 (2.3-fold), and *TOR* (4.2-fold) were significantly downregulated as compared to control in IR. A similar response was observed in BPT where a significant downregulation of ATG genes *viz. ATG 5* (2-fold), *8c* (3.5-fold) and *TOR* (2.9-fold) was noted, whereas the expression of *ATG1a* (0.4-fold), *3a* (1.6-fold), *7* (2.8-fold), *8b* (2-fold), *8d* (2-fold), *9a* (2.4-fold)increased 3h post salt stress in BPT. At 72h post salt treatment, the expression of *4a* (2.6-fold), *5* (2.2-fold), *12* (2.2-fold) and *TOR* (3.8-fold) were down-regulated while *ATG7* (1.5-fold), *8a* (1.7-fold), *8c* (2-fold), *8d* (2.6-fold), *8e* (1.7-fold), *9a* (5.2-fold), and *13b* (2.1-fold), were induced as

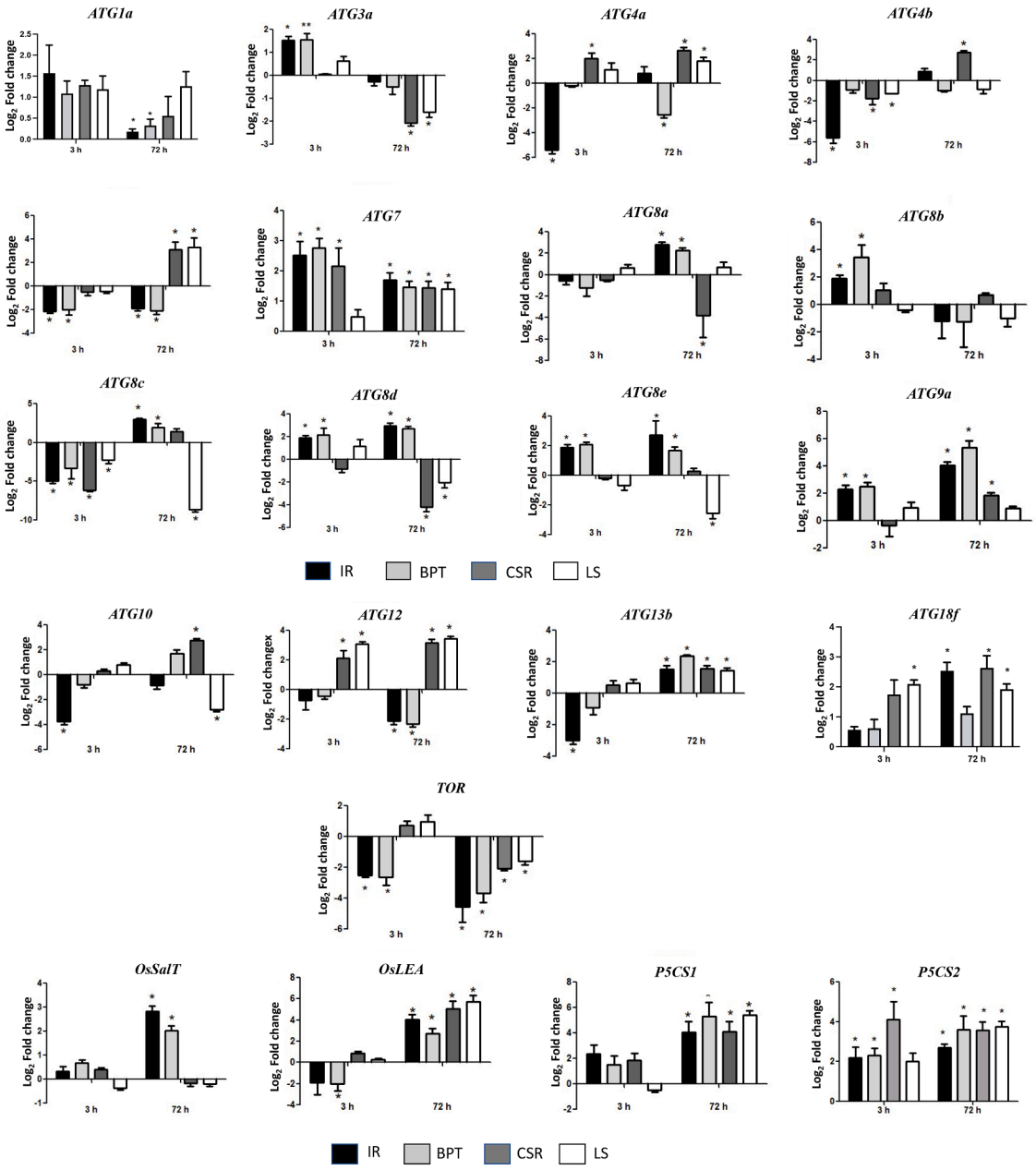


Fig. 4. Bars represent expression profile (relative expression in terms of Log_2 fold change with respect to control value for respective genotypes) of different autophagy related genes (*OsATGs*) and salt-stress responsive genes (*OsSalT, OsLEA, P5CS1* and *P5CS2*) in rice seedlings treated with NaCl for 3 and 72h. The asterisks (*) represent significant change at $p<0.05$ in comparison to respective control. The values presented are the mean ± SE of three independent biological and three technical replications.

compared to their respective controls in BPT. Among tolerant varieties, in CSR, in response to salt stress at 3h, a significant downregulation was observed in *ATG 4b* (1.9-fold), and *8c* (6.3-fold) *ATG4a* (2-fold), *7* (2.2-fold) and *12* (2-fold)showed a significant upregulation as compared to their respective controls. At 72h salt treatment in CSR, a significant upregulation was observed in *ATG 4a* (2.1-fold), *4b* (2.4-fold), *5* (3.1-fold), *7* (1.5-fold),*9a* (1.8-fold), *10* (2.7-fold), *12* (3.2-fold), *13b* (1.4-fold), *18f* (2.6-fold), however *3a* (2.07-fold), *8a* (4-fold),*8d* (4.1-fold) and *TOR* (2-fold) were significantly downregulated as compared to their respective controls. In LS, at 3h salt treatment, a significant down-regulation was recorded for *4b* (1.5-fold), and *8c* (2.5-fold), and upregulation in *ATG12* (3.1-fold),and *ATG18f* (2-fold) as compared to their respective controls. At 72h, a significant downregulation was observed in *3a* (1.6-fold), *8c* (8.8-fold), *8d* (2-fold), *8e* (2.5-fold), *10* (2.7-fold) and *TOR* (1.8-fold). On the contrary a significant upregulation was recorded in *ATG4a (1.8-fold), 5* (3.3-fold), *7* (1.4-fold), *12* (3.6-fold), *13b* (1.2-fold) and *18f* (1.8-fold)

Among salt stress responsive genes (Fig. 4b), the expression of *OsSalT* did not show any significant change at 3h while at 72h, the expression was significantly induced in sensitive varieties IR (2.8-fold) and BPT (2-fold) as compared to their respective controls. The expression of another stress responsive gene *OsLEA* did not show any change at 3h post stress except BPT where its expression declined to 2-fold. At 72h, its expression was induced significantly in all the varieties though at different levels. The expression of proline synthesis genes *P5CS1* also showed no significant change in expression at 3h, while an increased expression was observed in all the varieties at 72h.The expression of P5CS2, increased in all the varieties at 3h except LS while at 72h post stress all the varieties

recorded a significantly increased expression.

3.3.3. Induction of ATG proteins in E. coli provides stress tolerance

To evaluate the effect of autophagy induction on stress tolerance, three *ATG* genes showing consistent reciprocal expression patterns in contrasting salt-tolerant varieties were chosen for further study. We overexpressed these proteins (*OsATG8d, OsATG5* and *OsATG12*) in a prokaryotic system *i.e. E.coli* and subjected it to salt and osmotic stress (Fig. 5a). We analysed the *E.coli* growth patterns by measuring the O.D. at 600 nm. It was interesting to see that bacteria harbouring any of the *ATG* genes showed noticeably improved growth under control as well as stress conditions. At 4h, the significant difference in the growth curve started appearing between the transformed *E.coli* and the wild type under control as well as under stress conditions. Interestingly, at the higher levels of stress (200 mM NaCl and 10 % PEG), the shift in the growth curve was much more prominent than at the lower levels of stress.

3.4. Analysis of miRNA sequencing data for the shoot samples of contrasting salt-tolerant varieties, CSR and BPT

Twelve small-RNA libraries from shoot samples of two contrasting rice cultivars (BPT, sensitive; CSR, tolerant) under control and 100 mM NaCl for 72 h were generated for high-throughput sequencing (three biological replicates per condition). A summary of per-library metrics is provided in Supplementary Table ST2a. After adapter trimming, >98 % of raw reads were retained across all libraries, and following quality control and length selection (19–35 nt), >93 % of reads per library were taken forward (Supplementary Table ST2b). The complete list of detected known miRNAs is provided in Supplementary Table ST3. To prevent cross-species mis annotation, we restricted quantification to known *Oryza sativa* (osa) miRNAs only, excluding non-osa entries. For downstream analyses, only those miRNAs detected in at least two biological replicates in at least one treatment group were retained (Supplementary Table ST4). Based on this filtering criterion, length distribution analysis revealed a dominant 21-nt class of known *osa-miRNAs* across all libraries (Fig. 6a). The curated *osa-miRNAs* were classified into 38 families based on mature-sequence similarity. Among these, the *osa-miR812* family comprised five members, *osa-miR1861* contained four members, and *osa-miR444* included three members (Fig. 6b).

The Venn diagram (Fig. 6c) analysis identified 55 known miRNAs that were detected across all libraries while few of them were uniquely expressed in BPT-T (1) and CSR-T (3). BPT-T uniquely expressed *osa-miR1860-3p* while CSR-T uniquely expressed *osa-miR5508, osa-miR3980a-5p* and *osa-miR5805*.

Under salt stress, the two rice cultivars showed markedly different miRNA expression patterns in their shoot tissues. All differential-expression statistics (log_2 fold change, *p* value, FDR) are based on data from three independent biological replicates per condition. Under salt stress in comparison to control, 9 miRNAs (*osa-miR1432-5p, osa-miR1860-3p, osa-miR1871, osa-miR1861h, osa-miR1861e, osa-miR531a, osa-miR2879, osa-miR5513* and *osa-miR1874-3p*) were identified in BPT as differentially upregulated in the range of Log_2 FC of 5-6 fold. Similarly, under salt stress in CSR, *osa-miR3980a-5p* was up-regulated (Log_2 FC, 6.05), while 4 other miRNAs (*osa-miR812n-5p, osa-miR1861e, osa-miR1874-3p* and *osa-miR1861a*) were down-regulated (Log_2 FC, -5.99 to -7.55) in comparison to the control. The complete

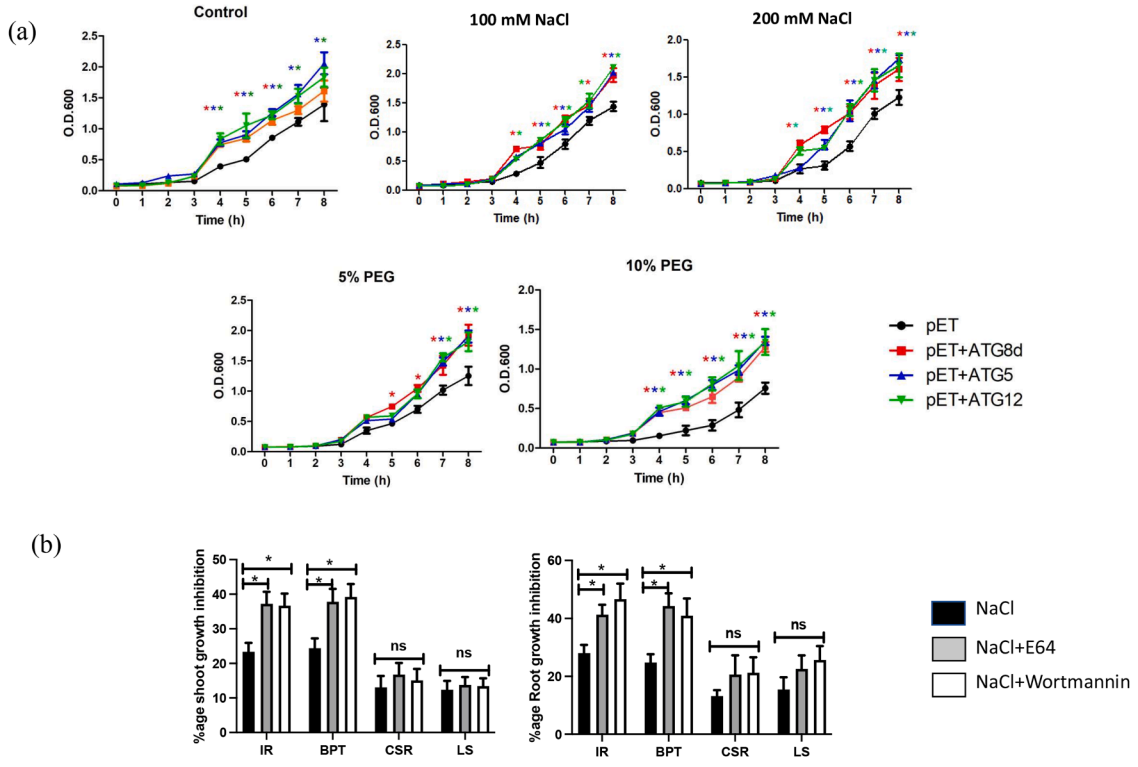


Fig. 5. (a) Line graphs representing the growth curve for *E.coli* transformed with empty pET28 vector and pET28 vector harbouring *OsATG8d, OATG5* and *OsATG12*. Bacterial culture was grown on media containing (a) MS media, and MS media supplemented with (Control) (b) 100 mM NaCl (c) 200 mM NaCl (d) 5 % PEG and (e) 10 % PEG. O.D. at 600 nm was recorded at different time points and plotted as growth curve. The starting viable cell density was similar for all cultures. The values presented are the mean ± SE of three independent biological and three technical replications. The asterisks *,**,*** represent significant change at $p<0.05$, $p<0.01$ and $p<0.001$ in comparison to the empty vector control. Data represent mean ± S.E of three independent biological replicates. (b) Impact of autophagy inhibition on percentage shoot and root growth inhibition in salt-sensitive (IR, BPT) and salt-tolerant (CSR, LS) rice varieties under salt stress. The bar graphs depict the percentage inhibition of shoot and root growth under 100 mM NaCl alone and in combination with autophagy inhibitors E64 (10 μM) and Wortmannin (5 μM) with respect to control conditions.

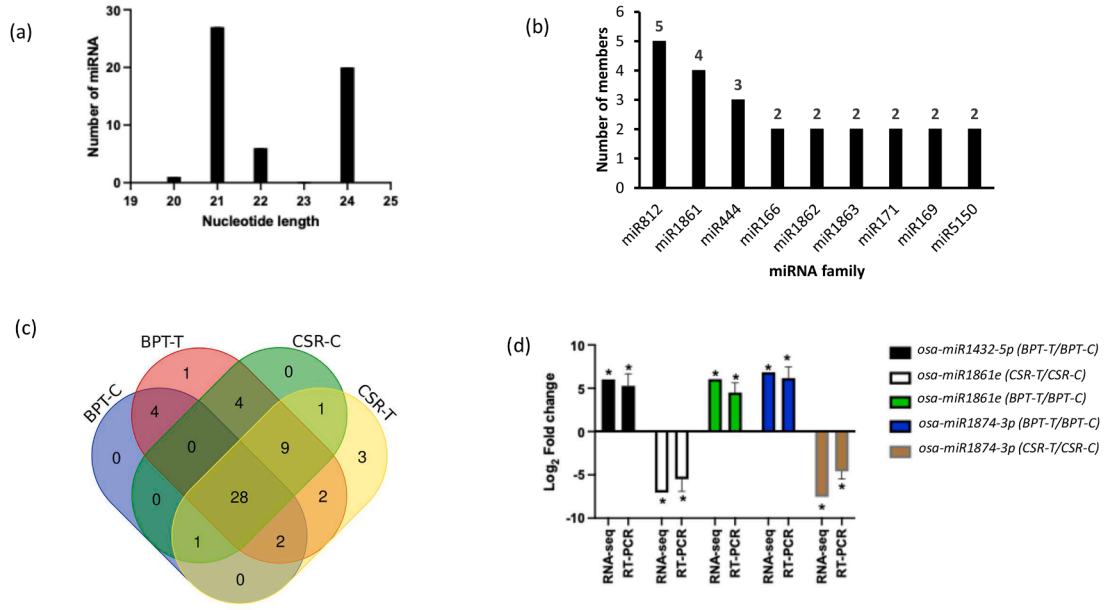


Fig. 6. Analysis of miRNAs from small RNA libraries of rice seedlings treated with or without NaCl. (a) Length distribution of miRNAs in BPT and CSR varieties under control (C) and salt-treated (T) conditions. (b) Families of identified miRNAs in BPT and CSR samples, with *miR1861* and *miR812* being the most abundant. Venn diagram showing the overlap of (c) known miRNAs in different categories of control and salt treated CSR and BPT (d) represents validation of differentially expressed miRNAs in RNA-seq analysis using qPCR in salt-treated rice varieties. The Log_2 fold change in expression levels of three miRNAs (*osa-miR1432-5p, osa-miR1874* and *osa-miR1861e)* is shown for RNA-seq and qPCR. Log_2 fold change for RNA-seq data was calculated as Log_2 (Transcript per million, TPM under salt stress / normalized TPM under control), while the log_2 fold change for qRT-PCR data was calculated with ΔΔCT method within the comparison groups. Error bars indicate standard error across biological replicates. Asterisks denote statistically significant differences ($p < 0.05$) between treated and control samples.

list of the DE-miRNAs with a p-value of ≤0.05 and their read count is provided in supplementary table ST5 and ST6.

3.4.1. *Prediction of target genes of differently expressed miRNAs*

Target prediction was done for all the known miRNAs identified (ST7). Supplementary table ST8 provides information for targets of all the differentially expressed miRNAs that are targeting genes with known biological functions. For further details on the binding sites, with target alignments and inhibition type, predicted targets of all the miRNAs identified are provided in table ST5. Many DE-miRNA have been found to target genes encoding proteins for autophagy and cellular degradation pathways (ATG11, TOR, E3 ubiquitin-protein ligase and transferases, Ubiquitin carboxyl-terminal hydrolase 26 (UBP26)), cellular transporters (potassium transporter, Cl^- channel protein, calcium-transporting ATPase, sugar transporter SWEET, phosphate transporter, MOT2 also known as Mitochondrial Outer membrane Translocase 2, magnesium transporter etc.). Several stress-responsive proteins and transcription factors including ionic stress response protein Plasma

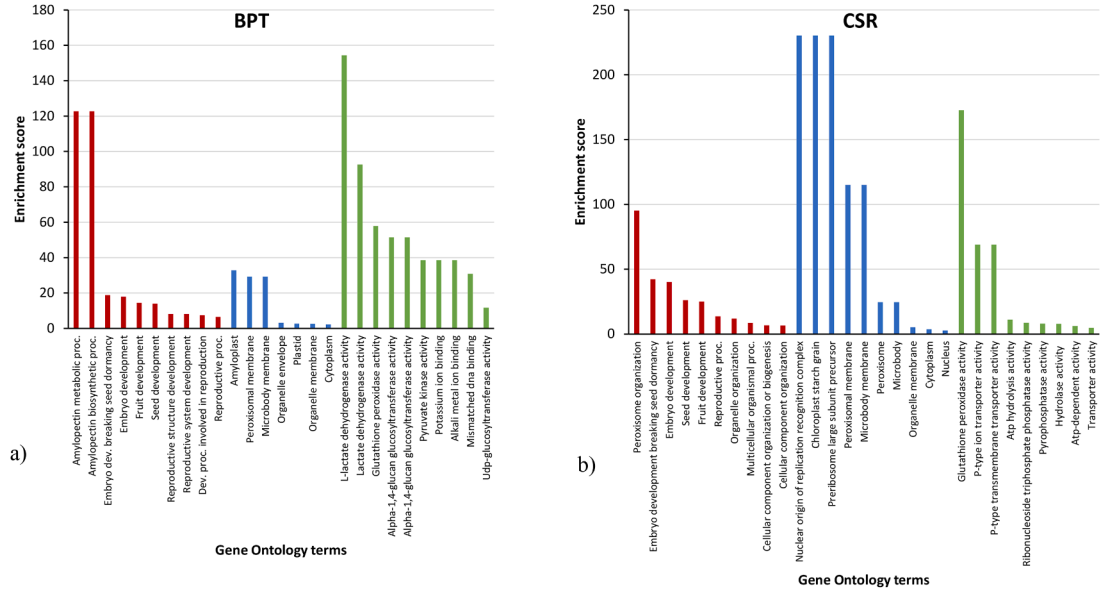


Fig. 7. Gene Ontology (GO) analysis of differentially expressed miRNAs in BPT and CSR rice varieties under salt stress. GO enrichment analysis in BPT (a) and CSR (b) under salt stress, categorized into three domains: Biological processes (BP) depicted by red histograms, Cellular components (CC) depicted by blue histograms and Molecular functions (MF) depicted by green histograms.

membrane H⁺-ATPase, protein heat stress transcription factor Spl7, WRKY66, Glutathione peroxidase, Salt Tolerance Receptor-like Cytoplasmic Kinase 1 (STKR1) etc. GO enrichment analysis revealed distinct transcriptional patterns between the salt-sensitive (BPT) and salt-tolerant (CSR) lines (Fig. 7). In BPT, enriched GO categories corresponded to down-regulated genes, due to their up-regulated cognate miRNAs, and were primarily linked to amylopectin metabolism, embryo/seed development and other growth related processes, indicating repression of growth programs under salinity. In CSR, all but one differentially expressed miRNA were down-regulated, suggesting de-repression of their targets. In contrast, CSR displayed enrichment of genes related to peroxisome organization, organelle biogenesis, antioxidant defense, and ion transport, reflecting transcriptional investment in maintaining cellular homeostasis. Enrichment of glutathione peroxidase and P-type ion transporter activities in CSR indicates enhanced ROS detoxification and ion balance.

3.4.2. Experimental validation of miRNA sequencing data

We selected three differentially expressed *osa-miRNAs viz. osa-miR1432-5p, osa-miR1874-3p,* and *osa-miR1861e* with predicted or previously reported targets in autophagy (e.g., *TOR*) and salt-adaptation pathways for stem-loop RT-qPCR validation. As shown in Fig. 6d, the direction (log2 fold-change trend) of RT-qPCR results was concordant with small RNA-seq, with expected differences in fold-change magnitude between platforms.

4. Discussion

4.1. Differential salt tolerance in rice varieties is governed by distinct physiological and ionic adaptations

Salinity imposes osmotic and ionic stress that dehydrates cells, reduces turgor and nutrient transport, and impairs photosynthesis, leading to stunted growth and yield loss (Arif et al., 2020; Rodríguez et al., 2023). In this study, the salt-sensitive varieties (IR and BPT) experienced more severe decline in growth parameters under salinity than the salt-tolerant varieties (CSR and LS). Leaf area remained unaffected in CSR and LS, pointing to the maintenance of cell turgor that is crucial for cell expansion and overall leaf growth (Neumann et al., 1988). Evidently, RWC which reflects hydration and cell turgor (González and González-Vilar, 2001), dropped only in IR and BPT, potentially causing membrane shrinkage and vulnerability to damage. This was corroborated by a compromised cell membrane integrity indicated by higher EL and lipid peroxidation, in sensitive varieties. Excess reactive oxygen species (ROS) likely contributed to this damage in IR and BPT, as evidenced by their elevated ROS levels and comparatively lower induction of antioxidant enzymes (SOD, CAT, POD) under salt stress. Consistent with this, salt-tolerant genotypes generally sustain essential physiological processes and avoid salt-induced disruptions, whereas sensitive genotypes succumb to the compounded stress factors (ionic toxicity, ROS, etc.) if not mitigated (Saini et al., 2021; Jin et al., 2025; Talakayala et al., 2025; Kaur et al., 2016c).

One prominent distinguishing trait between salt-tolerant and sensitive lines was proline accumulation. CSR and LS exhibited significantly higher proline levels even under control conditions, indicating a pre-emptive protective mechanism. Constitutively high proline enhances salt tolerance by stabilizing cellular structures, maintaining osmotic balance, and mitigating oxidative stress (Talakayala et al., 2025; Hayat et al., 2012; Kaur et al., 2016a). Under salt treatment, all varieties increased their proline content, but the sensitive BPT showed the greatest fold increase (reactive accumulation) while still not reaching the absolute proline concentrations of the tolerant lines. This implies that pre-existing proline pools in tolerant rice can sufficiently buffer 100 mM NaCl-induced osmotic stress, whereas sensitive rice must ramp up proline synthesis during stress, a response that may come too late or in insufficient amounts for full protection. The early (3h) and sustained (72h) upregulation of proline biosynthetic genes (*P5CS1, P5CS2*), which are involved in salt-tolerance in rice (Igarashi et al., 1997; Hur et al., 2004), in both genotype groups confirms activation of proline pathways, but the tolerant varieties' modest proline induction suggests their proactive osmotic adjustment reduced the need for extreme metabolic shifts. We also observed induction of other osmoprotection-related genes involved in salt tolerance such as *OsLEA* (late embryogenesis abundant) (Duan J and Cai, 2012) protein which was upregulated in all genotypes, consistent with its role as a molecular chaperone linked to long-term cellular protection (Ubaidillah et al., 2024) and *OsSalT* (salt-responsive protein) associated with ion homeostasis and osmoprotection (Kaur et al., 2022) which was induced at 72h in IR and BPT. Overall, osmolyte accumulation and membrane protection appears to be a priority in tolerant rice even before stress, providing a dominant first line of defence by maintaining cell turgor and mitigating ROS damage.

Ion homeostasis emerged as another primary determinant of tolerance. All varieties experienced increased Na^+ uptake in roots under salinity, but interestingly the tolerant LS accumulated significantly higher Na^+ in roots and shoots than the others. A similar pattern of increased Na^+ accumulation has been reported in other salt-tolerant crops such as wheat (Wu et al., 2015), barley (Shabala et al., 2010), mungbean (Talakayala et al., 2025) and lettuce (Bartha et al., 2015), in comparison to their respective sensitive varieties. Despite the common assumption that lower tissue Na^+ is always correlated with tolerance, certain salt-tolerant species (including some halophytes) can accumulate substantial Na^+ in roots and leaves, leveraging it for energy-efficient osmotic adjustment and potentially revealing higher tissue tolerance (Talakayala et al., 2025; Katschnig et al., 2015). The ultimate indicator of tissue tolerance is the ability to maintain chlorophyll pigment in the presence of high internal Na^+. Using a fixed 100 mM NaCl concentration, we observed that over time, tolerant varieties retained higher chlorophyll than the sensitive ones, especially beyond 24h. This chlorophyll retention, despite considerable Na^+ in tissues, suggests that LS effectively compartmentalize Na^+ away from chloroplasts and cytosol, thereby protecting the photosynthetic machinery. Notably, we found a parallel synergy between K^+ uptake and tissue tolerance. Tolerant LS showed markedly greater K^+ uptake in roots under salt, and both CSR and LS maintained higher shoot K^+ concentrations, K^+/Na^+ ratios and selective K^+ uptake than the sensitive lines suggesting that selective K^+ uptake could also be contributing to the higher tissue tolerance. Prior studies have also identified that the cellular K^+ retention is the most important hallmark of differential salinity tolerance (Liu et al., 2019; Kumari et al., 2021). Thus, LS and CSR's ability to preferentially uptake and transport K^+ helped preserve their cellular functions.

4.2. Autophagy is differentially induced in rice varieties differing in salt tolerance

Autophagy serves as a critical defense mechanism under stress, clearing damaged organelles and protein aggregates to maintain cellular homeostasis (Luo et al., 2017). Salinity induced autophagy in both tolerant and sensitive rice genotypes but to markedly different extents. MDC and LysoTracker staining revealed early autophagy activation at 3 h of salt exposure across all varieties, consistent with reports in *Arabidopsis* (Luo et al., 2017). By 72 h, autophagic structures accumulated more strongly in salt-sensitive lines (IR, BPT) than in tolerant ones (CSR, LS). This heightened response likely reflects greater cellular damage and oxidative stress in sensitive plants, necessitating elevated autophagy for survival. In contrast, tolerant genotypes, protected by stronger primary defenses, exhibited a moderate and regulated autophagic response. Collectively, these results suggest that autophagy functions as a secondary, damage-responsive pathway, intensely activated in sensitive rice to mitigate injury but only modestly engaged in tolerant lines whose proactive mechanisms limit cellular damage.

Expression patterns of autophagy regulators reflected the contrasting stress responses of the genotypes. Core autophagy-related (ATG) genes

together with the Target of Rapamycin (TOR) kinase constitute the central regulatory and execution machinery of the autophagy pathway (Xia et al., 2011; Maegawa et al., 2015). The protein kinase TOR, that inhibits ATG1/ATG13 phosphorylation (Liu and Bassham, 2010; Son et al., 2018), was more strongly repressed under salt stress in sensitive varieties. Correspondingly, core autophagy genes were more strongly induced in these genotypes. Members of the *ATG8* family (*b, d, e*), *ATG3a, ATG7*, and *ATG9a* that are involved in autophagosome formation and cargo degradation (Sharma et al., 2024), showed early upregulation (3 h) in sensitive plants, whereas tolerant ones displayed minimal or reduced induction, consistent with limited autophagic activity observed via live-cell imaging. By 72 h, transcriptional activation of several *ATG* components persisted in sensitive lines, while tolerant varieties showed induction of a distinct subset (*ATG4A, ATG5, ATG12*), along with some commonly regulated genes. This divergence suggests that sensitive and tolerant rice varieties engage different autophagy modules, possibly reflecting variation in flux efficiency or non-canonical autophagy functions. Interestingly, *ATG8d, ATG12*, and *ATG5* displayed contrasting expression patterns between tolerant and sensitive varieties at 72 h. *ATG8d* was upregulated in sensitive lines but downregulated in tolerant ones, suggesting transcriptional control in the former and possible post-translational activation (e.g., ATG8 deacetylation) in the latter (Huang et al., 2015). Elevated *ATG4* expression and reduced oxidative stress in tolerant varieties further support an ATG4-mediated post-translational regulation of ATG8, as ATG4 activity is redox-dependent and inhibited by oxidative stress (Perez-Perez et al., 2014, 2016; Yu et al., 2012). In contrast, *ATG5* and *ATG12* were induced in tolerant but repressed in sensitive lines, consistent with their known roles in promoting autophagy flux and stress tolerance (Minina et al., 2018; Chen et al., 2019). Heterologous expression of rice *ATG5, ATG8*, and *ATG12* in *E. coli* enhanced growth under NaCl and PEG stress (Fig. 5a), supporting their protective roles. As we observed a comparatively less induction of autophagy in live-cell imaging in tolerant lines as compared to sensitive ones, the upregulation of *ATG5* and *ATG12* in tolerant genotypes may also reflect autophagy-independent protective pathways, as ATG components have been implicated in non-canonical functions such as endocytosis, secretion, and developmental regulation (Nieto-Torres et al., 2021; Jia et al., 2019; Elander et al., 2023). Moreover, *in silico* promoter analysis (Supplementary Fig. S1) identified multiple stress- and hormone-responsive cis-acting regulatory elements in the upstream regions of *OsATG8d, OsATG5*, and *OsATG12*, including ABRE (abscisic acid–responsive element), ARE (anaerobic-responsive element), STRE (stress-responsive element), and DRE (dehydration-responsive element). Notably, all three promoters contain TGA motifs (auxin-responsive elements), ARE, and STRE, indicating shared regulatory inputs. Although each gene also harbours distinct cis-elements, the presence of these common motifs suggests coordinated regulation of these ATG genes in response to abiotic stress and hormone-mediated signalling.

To further evaluate the dependence on autophagy during salt stress tolerance, contrasting rice varieties were treated with autophagy inhibitors under 100 mM NaCl (Fig. 5b). Seedling growth was measured following treatments with NaCl alone or in combination with wortmannin (blocks early autophagosome formation; Blommaart et al., 1997) and E64 (inhibits late-stage autophagy; Moriyasu et al., 2008). Co-treatment with these inhibitors caused a stronger reduction in root and shoot growth in sensitive varieties, indicating a greater dependence on autophagy for maintaining cellular homeostasis under salt stress. Together, these findings position autophagy as a vital but secondary tolerance mechanism. It enhances salt tolerance by mitigating cellular stress, yet it is most beneficial when first-line defences are breached. As summarized in Fig. 8, salt-tolerant varieties primarily prevent injury through efficient osmotic adjustment (e.g., high basal proline), ROS detoxification, and selective ion regulation (high K^+/Na^+ balance), which limit the need for extensive autophagy. In contrast, sensitive varieties lacking these frontline defences undergo severe cellular

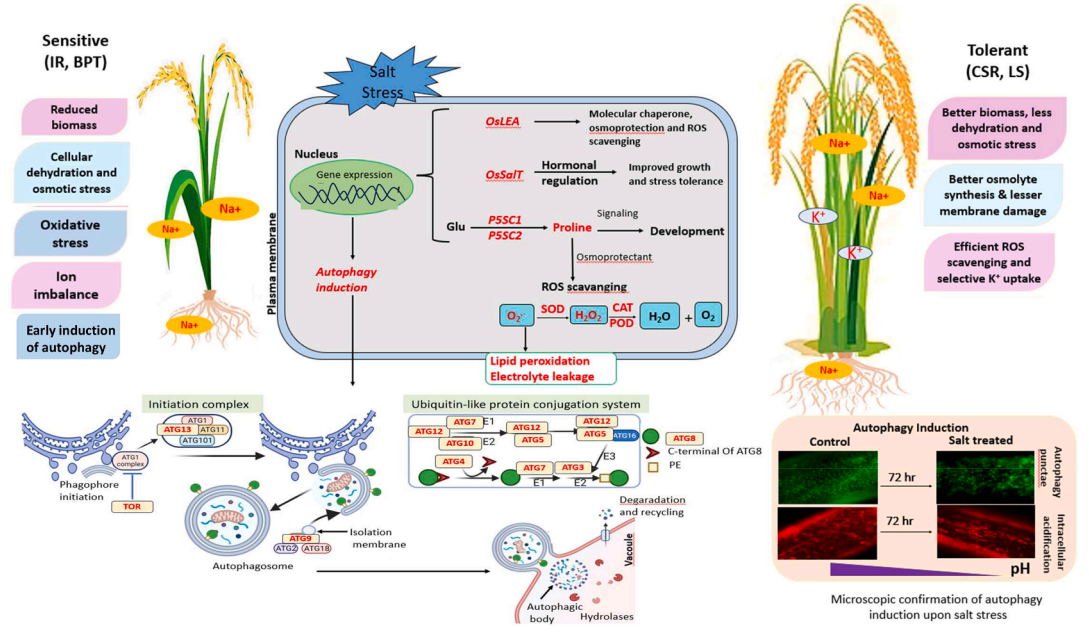


Fig. 8. The Fig. summarizes the contrasting strategies adopted by salt-sensitive and salt-tolerant rice varieties under salt stress. (Top Panel): Salt-sensitive varieties (IR, BPT) experience reduced biomass, cellular dehydration, oxidative stress, and ion imbalance. In contrast, salt-tolerant varieties (CSR, LS) maintain better biomass, osmotic regulation, efficient ROS scavenging, and selective potassium ion uptake, contributing to better growth and stress resilience. (Middle Panel): Changes in the expression of key genes involved various salt-stress responsive pathways assessed in this study, including the role of *OsLEA* (molecular chaperone), *OsSalT* (hormonal regulation and growth tolerance), and proline biosynthetic genes (*P5CS1, P5CS2*) in osmoprotection and ROS scavenging. (Bottom right Panel): Autophagy is induced as a defense mechanism to degrade damaged organelles and recycle cellular components under salt stress. Microscopic confirmation of autophagy induction upon salt stress, showing autophagic puncta and intracellular acidification after 72 hours of treatment. (Bottom Right Panel): Detailed schematic of autophagy pathway including autophagosome formation via the ubiquitin-like protein conjugation system, highlighting key regulatory components such as *TOR* and *ATG* genes. The expression of several of these have been observed to be regulated differently under salt stress in the present study.

damage, triggering extensive autophagy and other catabolic responses, a reactive strategy that alleviates stress but at the cost of growth.

4.3. *miRNA-mediated regulation differentially modulates stress-responsive pathways*

miRNAs add a post-transcriptional layer to salt-stress regulation (Islam et al., 2022). We compared miRNA profiles in tolerant vs. sensitive varieties to identify regulatory circuits underlying phenotypic divergence. Most known miRNAs belonged to the 21-nt category, potentially contributing to DNA methylation and chromatin modification leading to transcriptional silencing (Matzke et al., 2014). *miR-1861* and *miR-812* were the most abundant families across libraries which are broadly implicated in abiotic stress tolerance (Khare et al., 2023; Jeong et al., 2011) . Differential expression of multiple known miRNAs emerged in both varieties under salt stress. In CSR-T, *osa-miR-3980a* alone was upregulated in comparison to control CSR. It targets Salt Tolerance Receptor-Like Cytoplasmic Kinase 1(STRK1), which enhances salt tolerance by phosphorylating catalase to regulate H_2O_2 homeostasis (Zhou et al., 2018). This likely reflects feedback adjustment to already elevated antioxidant activity, allowing fine-tuning of ROS balance in the tolerant line. Several miRNAs were downregulated in CSR-T in comparison to CSR-C (e.g., *osa-miR-1874-3p, osa-miR-1861e*). *osa-miR-1874-3p* is associated with pollen development and grain filling (Wei et al., 2011). It likely targets salt-responsive *OsPEX11-1*, involved in peroxisome proliferation and ROS detoxification (Nayidu et al., 2008). *Osa-miR1874* is also potentially involved in improving the osmotic tolerance by targeting C2H2 zinc finger protein, by modulating the biosynthesis of osmotic substances (Kumar et al., 2024). *osa-miR-1861e* modulates Na^+ toxicity via *OsGST* and auxin transport (Khare et al., 2023). *Osa-miR1861e* is predicted to target genes encoding ubiquitin transferases, pectin acetylesterases, and glutathione peroxidases, suggesting its potential regulatory role at the interface of protein turnover, cell wall modification, and redox homeostasis under stress conditions. The expression of both the miRNAs is validated by stem-loop RT-PCR (Fig. 6d).

In BPT-T, nine miRNAs were upregulated compared to BPT-C. Among these, *osa-miR1432-5p* is predicted to target *TOR*, directly implicating it in the autophagy pathway. The qRT-PCR validation of both miRNA and TOR expression supports this regulatory connection, further strengthening the evidence that the increased autophagy observed in BPT-T samples may be modulated through this miRNA (Figs. 6d and 4b). In addition, *osa-miR1432-5p* is predicted to target potassium transporters, endopeptidase complexes, E3 ligases, and peroxiredoxins, and has been experimentally validated to target *OsACOT* (acyl-CoA thioesterase), where manipulation of this module alters grain filling and seed size (Zhao et al., 2019). *osa-miR1860-3p* is predicted to target trehalase and PP2A regulatory subunits, which are key regulators of osmotic adjustment and ROS detoxification (Yang et al., 2022; Rahikainen et al., 2016). Although its direct targets have not yet been experimentally validated, it has been repeatedly reported as stress-responsive (Mangrauthi et al., 2017). Similarly, *osa-miR1861h* is up-regulated that is predicted to target genes involved in raffinose synthase, chaperone protein ClpB3, pyruvate kinase, starch synthase, and ubiquitin carboxyl-terminal hydrolase 26. Overexpression of *osa-miR1861h* enhances salt tolerance, identifying it as a positive regulator of salinity adaptation(Ai et al., 2021). Both *osa-miR531a* and *osa-miR5513* are up-regulated and have been widely reported as drought-

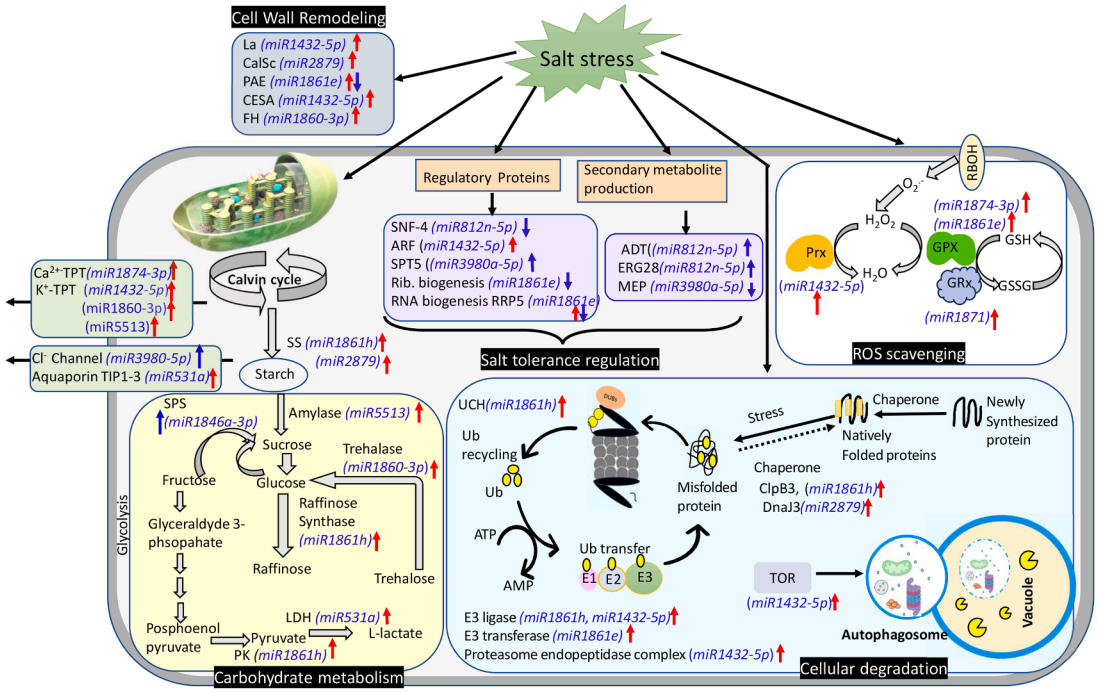


Fig. 9. Schematic representation of the predicted/empirically characterised targets of the differentially regulated miRNAs in BPT vs. CSR under salt stress. Red and blue arrows indicate the direction of regulation (up- or down-regulation) of miRNAs in the sensitive and tolerant varieties, respectively, compared to their corresponding controls. This diagram captures the interconnected pathways involved in rice responses to salt stress, differentiating between salt-sensitive and salt-tolerant varieties such as Cell Wall Remodeling enzymes (CESA PAE, Lac etc.), ion and metabolite transport (K^+-TPT, Cl^- channels), ROS-detoxifying enzymes (GPX, Prx, Grx), Carbohydrate Metabolism (SS, PK, SPS) Osmoprotectantion (trehalase and raffinose synthase), Protein Quality Control and Cellular Degradation involved ubiquitin-proteasome system, (UCH26, E3 ligase, ClpB3 for efficient protein turnover), Autophagy related (TOR). Abbreviations are explained here, Lac-Laccase; CalS-Callose synthase; FH-Formin-like; SYP- Syntaxin; PAE-Pectin acetylesterase;; K^+-TPT-Potassium transporter; Cl-Chloride channel; STRK1-Salt Tolerance-Related Kinase 1; GPX-Glutathione Peroxidase; GSH- Glutathione; GSSG- oxidized glutathione; SPS- Sucrose-Phosphate Synthase; PK- Pyruvate Kinase; SS- Sucrose Synthase; ClpB3-Caseinolytic Protease B3; PP2A- Protein Phosphatase 2A; TOR- Target of Rapamycin; DUBs-Deubiquitinating Enzymes, ADT-Arogenate dehydratase; ERG28-Ergosterol biosynthetic protein 28, MEP-2-C-methyl-D-erythritol-4-phosphate, GPX-Glutathione peroxidase; Prx-Peroxiredoxin; Grx-Glutaredoxin; LDH- L-Lactate Dehydrogenase; DnaJ3-Chaperone protein DnaJ 3 (an Hsp40/J-domain co-chaperone).

and heat-responsive, and are discussed in stress-priming studies; however, direct functional validation through overexpression or knockout studies remains to be established (*Kumar et al., 2024*). Collectively, our data indicate that salt stress elicits a differential reprogramming of miRNAs in tolerant and sensitive genotypes which may shape distict stress response in both the varieties. To integrate these effects, we mapped the differentially expressed miRNAs to their predicted or validated targets and associated physiological traits (Fig. 9). In the salt-sensitive line BPT, miRNA–target interactions pointed to a stress state marked by metabolic suppression and disrupted homeostasis. Downregulation of cell wall remodeling enzymes, carbohydrate-metabolic genes, and ion or water transporters likely restricts wall flexibility, osmolyte synthesis, and ionic balance. Repression of UPS elements, chaperones, and antioxidants further indicates weakened proteostasis and redox buffering, while TOR downregulation may promote compensatory autophagy. In contrast, the tolerant line CSR maintained active homeostasis, showing enhanced expression of aquaporins, antioxidants, and carbohydrate metabolism genes supporting osmoprotection, ROS detoxification, and energy supply. Upregulation of genes related to protein quality control, cell wall modification, and energy signaling suggests efficient remodeling and sustained growth under stress. GO enrichment analysis reinforces these trends as BPT exhibits suppression of developmental and metabolic pathways leading to growth inhibition, whereas CSR sustains transcriptional activation of redox, peroxisomal, and ion transport genes, enabling effective ROS detoxification and ionic balance. Together, these patterns highlight that CSR achieves tolerance through sustained homeostatic regulation, while BPT mounts a reactive, metabolically repressed response that fails to offset stress damage.

5. Conclusion

In conclusion, this study elucidates the distinct strategies adopted by rice varieties with contrasting salt tolerance. Salt-tolerance in CSR and LS is supported by enhanced antioxidant systems, osmotic adjustment, and ion homeostasis. Salt-sensitive varieties show earlier and stronger autophagy induction, likely reflecting greater cellular damage and stronger reliance on clearance mechanisms. We hypothesize that rice salt tolerance is governed by a three-layer hierarchy (1) Primary homeostasis maintained by early ion balance (high K^+/Na^+), tissue Na^+ sequestration, osmotic adjustment and membrane protection (proline/LEA), and ROS regulation potentially acts as the dominant upstream defence limiting initial damage. (2) Autophagy functions as a secondary, synergistic layer, with tolerant genotypes favouring an ATG4–ATG5–ATG12 module for efficient flux, whereas sensitive genotypes show stronger TOR repression and ATG8-driven massive autophagy to clear accumulated injury and (3) miRNA-mediated gating provides a third, fine-tuning layer that adjusts thresholds across ion transport, antioxidant capacity, and autophagy gene expression and coordinates these pathways. The novelty of this work thus lies in uncovering how salt stress orchestrates autophagy and miRNA pathways in concert to mediate differential salt tolerance in rice. The study offer candidates for experimental validation through transient assays, degradome sequencing, or CRISPR editing. Tissue-specific analysis of miRNA responses could further refine their functional roles.

Funding

IS thanks Department of Biotechnology, Govt. of India for funding assistance in the form of Ramalingaswami Fellowship (Grant no. BT/RLF/Re-entry/48/2018). IS also thanks, CSIR-CIMAP for the support. PBK is supported by the NASI-Platinum Jubilee Senior Scientist position. NK is thankful to the Department of Science and Technology, Government of India, for the financial assistance received under the DST-Woman Scientist-A (WOS-A) scheme (DST/WOS-A/LS-64/2020 (G)).

Data availability

The datasets generated during and/or analysed during the current study are available from the corresponding author on reasonable request.

CRediT authorship contribution statement

Ashwini Talakayala: Writing – original draft, Validation, Methodology, Investigation. **Navdeep Kaur:** Writing – original draft, Methodology. **Wricha Tyagi:** Writing – original draft, Methodology, Conceptualization. **Pratap Kumar Pati:** Writing – review & editing, Supervision, Conceptualization. **P.B. Kirti:** Writing – review & editing, Supervision, Conceptualization. **Isha Sharma:** Writing – original draft, Supervision, Project administration, Methodology, Investigation, Funding acquisition, Formal analysis, Conceptualization.

Declaration of competing interest

The authors have no relevant financial or non-financial interests to disclose

Supplementary materials

Supplementary material associated with this article can be found, in the online version, at doi:10.1016/j.stress.2025.101200.

References

Ai, B., Chen, Y., Zhao, M., Ding, G., Xie, J., Zhang, F., 2021. Overexpression of miR1861h increases tolerance to salt stress in rice (*Oryza sativa* L.). Genet. Resour. Crop Evol. 68, 87–92. https://doi.org/10.1007/s10722-020-01024-5.

Arif, Y., Singh, P., Siddiqui, H., et al., 2020. Salinity induced physiological and biochemical changes in plants: an omic approach towards salt stress tolerance. Plant Physiol. Biochem. 156, 64–77. https://doi.org/10.1016/j.plaphy.2020.08.042.

Arnon, D.I., 1949. Copper enzymes in isolated chloroplasts. Polyphenoloxidase in *Beta vulgaris*. Plant Physiol. 24, 1. https://doi.org/10.1104/pp.24.1.1.

Barrs, H.D., Weatherley, P.E., 1962. A re-examination of the relative turgidity technique for estimating water deficits in leaves. Aust. J. Biol. Sci. 15, 413–428. https://doi.org/10.15666/aeer/1604_42514263.

Bartha, C., Fodorpataki, L., Martinez-Ballesta, M.D.C., et al., 2015. Sodium accumulation contributes to salt stress tolerance in lettuce cultivars. J. Appl. Bot. Food Qual. 88, 42–48. https://doi.org/10.5073/JABFQ.2015.088.008.

Bates, L.S., Waldren, R.P., Teare, I.D., 1973. Rapid determination of free proline for water-stress studies. Plant Soil 39, 205–207. https://doi.org/10.1007/BF00018060.

Bin Rahman, A.R., Zhang, J., 2023. Trends in rice research: 2030 and beyond. Food Energy Secur. 12, e390. https://doi.org/10.1002/fes3.390.

Blommaart, E.F., Krause, U., Schellens, J.P., et al., 1997. The phosphatidylinositol 3-kinase inhibitors wortmannin and LY294002 inhibit autophagy in isolated rat hepatocytes. Eur. J. Biochem. 243, 240–246. https://doi.org/10.1111/j.1432-1033.1997.0240a.x.

Bradford, M.M., 1976. A rapid and sensitive method for the quantitation of microgram quantities of protein utilizing the principle of protein-dye binding. Anal. Biochem. 72, 248–254. https://doi.org/10.1016/0003-2697(76)90527-3.

Chance, B., Maehly, A.C., 1955. Assay of catalases and peroxidases. Methods Enzymol. 2, 764–775. https://doi.org/10.1016/S0076-6879(55)02300-8.

Chen, Q., Soulay, F., Saudemont, B., et al., 2019. Overexpression of ATG8 in *Arabidopsis* stimulates autophagic activity and increases nitrogen remobilization efficiency and grain filling. Plant Cell Physiol. 60, 343–352. https://doi.org/10.1093/pcp/pcy214.

Chen, T., Shabala, S., Niu, Y., et al., 2021. Molecular mechanisms of salinity tolerance in rice. Crop J. 9, 506–520. https://doi.org/10.1016/j.cj.2021.03.005.

Dejonghe, W., Sharma, I., Denoo, B., et al., 2019. Disruption of endocytosis through chemical inhibition of clathrin heavy chain function. Nat. Chem. Biol. 15, 641–649. https://doi.org/10.1038/s41589-019-0262-1.

Dhanyalakshmi, K.H., Nataraja, K.N., 2021. Universal stress protein-like gene from mulberry enhances abiotic stress tolerance in *Escherichia coli* and transgenic tobacco cells. Plant Biol. 23, 1190–1194. https://doi.org/10.1111/plb.13311.

Ding, T., Li, W., Li, F., et al., 2024. microRNAs: Key regulators in plant responses to abiotic and biotic stresses via endogenous and cross-kingdom mechanisms. Int. J. Mol. Sci. 25, 1154. https://doi.org/10.3390/ijms25021154.

Duan, J., Cai, W., 2012. *OsLEA3-2*, an Abiotic Stress Induced Gene of Rice Plays a Key Role in Salt and Drought Tolerance. PLoS ONE 7 (9), e45117. https://doi.org/10.1371/journal.pone.0045117.

Elander, P.H., Holla, S., Sabljic, I., et al., 2023. Interactome of *Arabidopsis* ATG5 suggests functions beyond autophagy. Int. J. Mol. Sci. 24, 12300. https://doi.org/10.3390/ijms241512300.

FAO, 2024. Global rice production to reach record 543.6 million tonnes in 2024/25. Food and Agriculture Organization of the United Nations [URL] (accessed 21 October 2025).
Formey, D., Sallet, E., Lelandais-Brière, C., et al., 2014. The small RNA diversity from *Medicago truncatula* roots under biotic interactions evidences the environmental plasticity of the miRNAome. Genome Biol. 15, 457. https://doi.org/10.1186/s13059-014-0457-4.
Giannopolitis, C.N., Ries, S.K., 1977. Superoxide dismutases: I. Occurrence in higher plants. Plant Physiol. 59, 309–314. https://doi.org/10.1104/pp.59.2.309.
González, L., González-Vilar, M., 2001. Determination of relative water content. In: Reigosa, M.J. (Ed.), Handbook of Plant Ecophysiology Techniques. Springer, Dordrecht, pp. 207–212. https://doi.org/10.1007/0-306-48057-3_14.
Goswami, K., Tripathi, A., Sanan-Mishra, N., 2017. Comparative miRomics of salt-tolerant and salt-sensitive rice. J. Integr. Bioinform. 14, 20170002. https://doi.org/10.1515/jib-2017-0002.
Grellet Bournonville, C.F., Díaz-Ricci, J.C., 2011. Quantitative determination of superoxide in plant leaves using a modified NBT staining method. Phytochem. Anal. 22, 268–271. https://doi.org/10.1002/pca.1275.
Hasan, M.M., Rahman, M.A., Corpas, F.J., et al., 2024. Salt stress tolerance in rice (*Oryza sativa* L.): a proteomic overview of recent advances and future prospects. Plant Stress 11, 100307. https://doi.org/10.1016/j.stress.2023.100307.
Hayat, S., Hayat, Q., Alyemeni, M.N., et al., 2012. Role of proline under changing environments: a review. Plant Signal. Behav. 7, 1456–1466. https://doi.org/10.4161/psb.21949.
Hodges, D.M., DeLong, J.M., Forney, C.F., Prange, R.K., 1999. Improving the thiobarbituric acid-reactive-substances assay for estimating lipid peroxidation in plant tissues containing anthocyanin and other interfering compounds. Planta 207, 604–611. https://doi.org/10.1007/s004250050524.
Huang, R., Xu, Y., Wan, W., et al., 2015. Deacetylation of nuclear LC3 drives autophagy initiation under starvation. Mol. Cell 57, 456–466. https://doi.org/10.1016/j.molcel.2014.12.013.
Hur, J., Jung, K.H., Lee, C.H., An, G., 2004. Stress-inducible OsP5CS2 gene is essential for salt and cold stress tolerance in rice. Plant Sci. 166, 741–749.
Igarashi, Y., Yoshiba, Y., Sanada, Y., Yamaguchi-Shinozaki, K., Wada, K., Shinozaki, K., 1997. Characterization of the gene for Δ^1-pyrroline-5-carboxylate synthetase and correlation between the expression of the gene and salt tolerance in *Oryza sativa* L. Plant Molecular Bio. 33, 857–865.
Islam, W., Waheed, A., Naveed, H., Zeng, F., 2022. MicroRNAs mediated plant responses to salt stress. Cells 11, 2806. https://doi.org/10.3390/cells11182806.
Jeong, D.H., Park, S., Zhai, J., Gurazada, S.G., De Paoli, E., Meyers, B.C., et al., 2011. Massive analysis of rice small RNAs: mechanistic implications of regulated microRNAs and variants for differential target RNA cleavage. Plant Cell 23, 4185–4207. https://doi.org/10.1105/tpc.111.089045.
Jia, M., Liu, X., Xue, H., et al., 2019. Noncanonical ATG8–ABS3 interaction controls senescence in plants. Nat. Plants 5, 212–224. https://doi.org/10.1038/s41477-018-0348-x.
Jiang, J., Zhu, H., Li, N., et al., 2022. The miR393-target module regulates plant development and responses to biotic and abiotic stresses. Int. J. Mol. Sci. 23, 9477. https://doi.org/10.3390/ijms23169477.
Jin, D., Xu, Y., Iqbal, A., et al., 2025. Comparative transcriptome and hormonal analysis reveals the mechanisms of salt tolerance in rice. Int. J. Mol. Sci. 26, 6660. https://doi.org/10.3390/ijms26146660.
Jones, J.J., Wolf, B., Mills, H.A., 1991. Plant Analysis Handbook: A Practical Sampling, Preparation, Analysis, and Interpretation Guide. Micro-Macro Publishing Inc., Athens, GA.
Katschnig, D., Bliek, T., Rozema, J., Schat, H., 2015. Constitutive high-level SOS1 expression and absence of HKT1;1 expression in the salt-accumulating halophyte *Salicornia dolichostachya*. Plant Sci. 234, 144–154. https://doi.org/10.1016/j.plantsci.2015.02.011.
Kaur, N., Dhawan, M., Sharma, I., Pati, P.K., 2016c. Interdependency of reactive oxygen species generating and scavenging system in salt sensitive and salt tolerant cultivars of rice. BMC Plant Biol. 16, 1–13. https://doi.org/10.1186/s12870-016-0824-2.
Kaur, N., Kirat, K., Saini, S., et al., 2016a. Reactive oxygen species generating system and brassinosteroids are linked to salt stress adaptation mechanisms in rice. Plant Signal. Behav. 11, e1247136. https://doi.org/10.1080/15592324.2016.1247136.
Kaur, N., Pati, P.K., 2017. Integrating classical with emerging concepts for better understanding of salinity stress tolerance mechanisms in rice. Front. Environ. Sci. 5, 42. https://doi.org/10.3389/fenvs.2017.00042.
Kaur, N., Prashanth, K.H., Bhatti, M.S., Pati, P.K., 2022. *OsSalT* gene cloned from rice provides evidence of its role in salinity and drought stress tolerance. Plant Sci. 320, 111306. https://doi.org/10.1016/j.plantsci.2022.111306.
Kaur, N., Sharma, I., Kirat, K., Pati, P.K., 2016b. Detection of reactive oxygen species in *Oryza sativa* L. (rice). Bio-protocol 6, e2061. https://doi.org/10.21769/BioProtoc.2061.
Khare, T., Barvkar, V.T., Devarumath, R.M., Kumar, V., 2023. *Osa*-miR1861e modulates sodium toxicity responses in rice immature grains via *OsGST* and *OsPILS7b*. J. Plant Growth Regul. https://doi.org/10.1007/s00344-023-11193-8.
Kumar, D., Mulani, E., Singh, B.K., et al., 2024. Understanding the role of miRNAs in governing the drought sensitive response of a rice mega variety, Swarna at reproductive stage. Plant Stress 11, 100302. https://doi.org/10.1016/j.stress.2024.100302.
Kumari, S., Chhillar, H., Chopra, P., et al., 2021. Potassium: a track to develop salinity tolerant plants. Plant Physiol. Biochem. 167, 1011–1023. https://doi.org/10.1016/j.plaphy.2021.09.031.
Li, C., Lu, C., Zou, B., et al., 2022. Genome-wide association study reveals a genetic mechanism of salt tolerance germinability in rice (*Oryza sativa* L.). Front. Plant Sci. 13, 934515. https://doi.org/10.3389/fpls.2022.934515.
Li, Y., Cao, X.L., Zhu, Y., et al., 2019. *Osa*-miR398b boosts H_2O_2 production and rice blast disease-resistance via multiple superoxide dismutases. New Phytol. 222, 1507–1522. https://doi.org/10.1111/nph.15663.
Li, Y., Xu, X., Qi, G., et al., 2023. Mechanisms of autophagy function and regulation in plant growth, development, and response to abiotic stress. Crop J. 11, 1611–1625. https://doi.org/10.1016/j.cj.2023.09.005.
Liu, J., Shabala, S., Shabala, L., et al., 2019. Tissue-specific regulation of Na^+ and K^+ transporters explains genotypic differences in salinity stress tolerance in rice. Front. Plant Sci. 10, 1361. https://doi.org/10.3389/fpls.2019.01361.
Liu, Y., Bassham, D.C., 2010. TOR is a negative regulator of autophagy in *Arabidopsis thaliana*. PLoS One 5, e11883. https://doi.org/10.1371/journal.pone.0011883.
Liu, Y., Xiong, Y., Bassham, D.C., 2009. Autophagy is required for tolerance of drought and salt stress in plants. Autophagy 5, 954–963. https://doi.org/10.4161/auto.5.7.9290.
Luo, L., Zhang, P., Zhu, R., et al., 2017. Autophagy is rapidly induced by salt stress and is required for salt tolerance in *Arabidopsis*. Front. Plant Sci. 8, 1459. https://doi.org/10.3389/fpls.2017.01459.
Mangrauthia, S.K., Bhogireddy, S., Agarwal, S., et al., 2017. Genome-wide changes in microRNA expression during short and prolonged heat stress and recovery in contrasting rice cultivars. J. Exp. Bot. 68, 2399–2412. https://doi.org/10.1093/jxb/erx111.
Matzke, M.A., Mosher, R.A., 2014. RNA-directed DNA methylation: an epigenetic pathway of increasing complexity. Nat. Rev. Genet. 15, 394–408. https://doi.org/10.1038/nrg3683.
Maegawa, K., Takii, R., Ushimaru, T., Kozaki, A., 2015. Evolutionary conservation of TORC1 components, TOR, Raptor, and LST8, between rice and yeast. Mol. Genet Genom. 290 (5), 2019–2030. https://doi.org/10.1007/s00438-015-1056-0. OctEpub 2015 May 9. PMID: 25956502.
Minina, E.A., Moschou, P.N., Vetukuri, R.R., et al., 2018. Transcriptional stimulation of rate-limiting components of the autophagic pathway improves plant fitness. J. Exp. Bot. 69, 1415–1432. https://doi.org/10.1093/jxb/ery010.
Moriyasu, Y., Inoue, Y., 2008. Use of protease inhibitors for detecting autophagy in plants. Methods Enzymol. 451, 557–580. https://doi.org/10.1016/S0076-6879(08)03232-3.
Nayidu, N.K., Wang, L., Xie, W., et al., 2008. Comprehensive sequence and expression profile analysis of *PEX11* gene family in rice. Gene 412, 59–70. https://doi.org/10.1016/j.gene.2008.01.006.
Neumann, P.M., Van Volkenburgh, E., Cleland, R.E., 1988. Salinity stress inhibits bean leaf expansion by reducing turgor, not wall extensibility. Plant Physiol. 88, 233–237. https://doi.org/10.1104/pp.88.1.233.
Nguyen, D.Q., Nguyen, N.L., Nguyen, V.T., et al., 2023. Comparative analysis of microRNA expression profiles in shoot and root tissues of contrasting rice cultivars (*Oryza sativa* L.) with different salt stress tolerance. PLoS One 18, e0286140. https://doi.org/10.1371/journal.pone.0286140.
Nieto-Torres, J.L., Leidal, A.M., Debnath, J., Hansen, M., 2021. Beyond autophagy: the expanding roles of ATG8 proteins. Trends Biochem. Sci. 46, 673–686. https://doi.org/10.1016/j.tibs.2021.01.004.
Parmar, S., Gharat, S.A., Tagirasa, R., et al., 2020. Identification and expression analysis of miRNAs and elucidation of their role in salt tolerance in rice varieties susceptible and tolerant to salinity. PLoS One 15, e0230958. https://doi.org/10.1371/journal.pone.0230958.
Pathak, H., Parameswaran, C., Subudhi, H.N., et al., 2019. Rice varieties of NRRI: yield, quality, special traits and tolerance to biotic & abiotic stresses. NRRI Res. Bull. 20, 68. ICAR–National Rice Research Institute, Cuttack, Odisha. https://krishikosh.egranth.ac.in/handle/1/5810213934. accessed 21 October 2025.
Pérez-Pérez, M.E., Lemaire, S.D., Crespo, J.L., 2016. Control of autophagy in *Chlamydomonas* is mediated through redox-dependent inactivation of the ATG4 protease. Plant Physiol. 172, 2219–2234. https://doi.org/10.1104/pp.16.01582.
Pérez-Pérez, M.E., Zaffagnini, M., Marchand, C.H., Crespo, J.L., Lemaire, S.D., 2014. The yeast autophagy protease Atg4 is regulated by thioredoxin. Autophagy 10, 1953–1964. https://doi.org/10.4161/auto.34396.
Prashanth, C., Mahantashivayogayya, K., Diwan, J.R., et al., 2020. Genetic variability and association studies on Bpt-5204 based rice mutants under saline stress soil. Int. J. Curr. Microbiol. Appl. Sci. 9, 2441–2450. https://doi.org/10.20546/ijcmas.2020.902.279.
Rahikainen, M., Pascual, J., Alegre, S., et al., 2016. PP2A phosphatase as a regulator of ROS signaling in plants. Antioxidants 5, 8. https://doi.org/10.3390/antiox5010008.
Rai, M., Chucha, D., Deepika, D., et al., 2023. Pyramiding of qDTY1.1 and qDTY3.1 into rice mega-variety Samba Mahsuri-Sub1: physiological performance under water deficit conditions. Physiol. Mol. Biol. Plants 29, 1931–1943. https://doi.org/10.1007/s12298-023-01387-5.
Rawal, H.C., Ali, S., Mondal, T.K., 2023. Role of non-coding RNAs against salinity stress in *Oryza* species: strategies and challenges in analyzing miRNAs, tRFs and circRNAs. Int. J. Biol. Macromol. 242, 125172. https://doi.org/10.1016/j.ijbiomac.2023.125172.
Rodríguez Coca, L.I., García González, M.T., Gil Unday, Z., et al., 2023. Effects of sodium salinity on rice (*Oryza sativa* L.) cultivation: a review. Sustainability 15, 1804. https://doi.org/10.3390/su15031804.
Saini, S., Kaur, N., Marothia, D., et al., 2021. Morphological analysis, protein profiling and expression analysis of auxin homeostasis genes of roots of two contrasting cultivars of rice provide inputs on mechanisms involved in rice adaptation towards salinity stress. Plants 10, 1544. https://doi.org/10.3390/plants10081544.

Shabala, S., Shabala, L., Cuin, T.A., et al., 2010. Xylem ionic relations and salinity tolerance in barley. Plant J 61, 839–853. https://doi.org/10.1111/j.1365-313X.2009.04110.x.

Sharma, I., Ching, E., Saini, S., et al., 2013. Exogenous application of brassinosteroid offers tolerance to salinity by altering stress responses in rice variety Pusa Basmati-1. Plant Physiol. Biochem. 69, 17–26. https://doi.org/10.1016/j.plaphy.2013.04.013.

Sharma, I., Kirti, P.B., Pati, P.K., 2022. Autophagy: a game changer for plant development and crop improvement. Planta 256, 103. https://doi.org/10.1007/s00425-022-04004-z.

Sharma, I., Talakayala, A., Tiwari, M., et al., 2024. A synchronized symphony: intersecting roles of ubiquitin proteasome system and autophagy in cellular degradation. Plant Physiol. Biochem., 108700 https://doi.org/10.1016/j.plaphy.2024.108700.

Signorelli, S., Tarkowski, Ł.P., Van den Ende, W., Bassham, D.C., 2019. Linking autophagy to abiotic and biotic stress responses. Trends Plant Sci. 24, 413–430. https://doi.org/10.1016/j.tplants.2019.02.001.

Singh, R., Singh, Y., Xalaxo, S., et al., 2016. From QTL to variety—harnessing the benefits of QTLs for drought, flood and salt tolerance in mega rice varieties of India through a multi-institutional network. Plant Sci. 242, 278–287. https://doi.org/10.1016/j.plantsci.2015.08.008.

Son, O., Kim, S., Kim, D., et al., 2018. Involvement of TOR signaling motif in the regulation of plant autophagy. Biochem. Biophys. Res. Commun. 501, 643–647. https://doi.org/10.1016/j.bbrc.2018.05.027.

Talakayala, A., Jupally, Y., Asinti, S., et al., 2025. Differences in the regulation of ion imbalance in response to high Na^+ load hint at differential strategies for salt-tolerance in mungbean genotypes (*Vigna radiata* L.). Plant Growth Regul. 105, 89–109. https://doi.org/10.1007/s10725-024-01257-4.

Tiwari, S., Jain, M., Singla-Pareek, S.L., Bhalla, P.L., Singh, M.B., Pareek, A., 2023. Pokkali: a naturally evolved salt-tolerant rice shows a distinguished set of lncRNAs possibly contributing to the tolerant phenotype. Int. J. Mol. Sci. 24, 11677. https://doi.org/10.3390/ijms241411677.

Tong, H., Wang, C., Han, X., et al., 2025. Multi-omics-based construction of ncRNA–gene–metabolite networks provides new insights into metabolic regulation under salt stress in rice. Rice 18, 50. https://doi.org/10.1186/s12284-025-00811-6.

Ubaidillah, M., Farooq, M., Kim, K.M., 2024. Enhancing salt tolerance in rice genotypes through exogenous melatonin application by modulating growth patterns and antistress agents. Sci. Rep. 14, 25217. https://doi.org/10.1038/s41598-024-77161-8.

Velikova, V., Yordanov, I., Edreva, A., 2000. Oxidative stress and some antioxidant systems in acid rain-treated bean plants: protective role of exogenous polyamines. Plant Sci. 151, 59–66. https://doi.org/10.1016/S0168-9452(99)00197-1.

Wei, L.Q., Yan, L.F., Wang, T., 2011. Deep sequencing on genome-wide scale reveals the unique composition and expression patterns of microRNAs in developing pollen of *Oryza sativa*. Genome Biol. 12, R53. https://doi.org/10.1186/gb-2011-12-6-r53.

Wu, H., Shabala, L., Liu, X., et al., 2015. Linking salinity stress tolerance with tissue-specific Na^+ sequestration in wheat roots. Front. Plant Sci. 6, 71. https://doi.org/10.3389/fpls.2015.00071.

Wu, W., Zhang, Q., Ervin, E.H., et al., 2017. Physiological mechanism of enhancing salt stress tolerance of perennial ryegrass by 24-epibrassinolide. Front. Plant Sci. 8, 1017. https://doi.org/10.3389/fpls.2017.01017.

Xia, K., Liu, T., Ouyang, J., et al., 2011. Genome-wide identification, classification, and expression analysis of autophagy-associated gene homologues in rice (*Oryza sativa* L.). DNA Res. 18, 363–377. https://doi.org/10.1093/dnares/dsr024.

Yadav, N.S., Singh, V.K., Singh, D., Jha, B., 2014. A novel gene *SbSI-2* encoding nuclear protein from a halophyte confers abiotic stress tolerance in *E. coli* and tobacco. PLoS One 9, e101926. https://doi.org/10.1371/journal.pone.0101926.

Yang, Y., Yao, Y., Li, J., et al., 2022. Trehalose alleviated salt stress in tomato by regulating ROS metabolism, photosynthesis, osmolyte synthesis, and trehalose metabolic pathways. Front. Plant Sci. 13, 772948. https://doi.org/10.3389/fpls.2022.772948.

Yu, Z.Q., Ni, T., Hong, B., et al., 2012. Dual roles of Atg8–PE deconjugation by Atg4 in autophagy. Autophagy 8, 883–892. https://doi.org/10.4161/auto.19652.

Yuan, H., Cheng, M., Wang, R., et al., 2024. miR396b/GRF6 module contributes to salt tolerance in rice. Plant Biotechnol. J. 22, 2079–2092. https://doi.org/10.1111/pbi.14326.

Zhou, Y.B., Liu, C., Tang, D.Y., et al., 2018. The receptor-like cytoplasmic kinase STRK1 phosphorylates and activates CatC, thereby regulating H_2O_2 homeostasis and improving salt tolerance in rice. Plant Cell 30, 1100–1118.